A bacterial TIR-based immune system senses viral capsids to initiate defense

Cameron G. Roberts[1,#*], Chloe B. Fishman[1,#], Dalton V. Banh and Luciano A. Marraffini[1,2*]

[1]Laboratory of Bacteriology, The Rockefeller University, 1230 York Ave, New York, NY 10065, USA.

[2]Howard Hughes Medical Institute, The Rockefeller University, 1230 York Ave, New York, NY 10065, USA.

[#]these authors contributed equally to this study.

*Correspondence to: croberts@rockefeller.edu, marraffini@rockefeller.edu

ABSTRACT

Toll/interleukin-1 receptor (TIR) domains are present in immune systems that protect prokaryotes from viral (phage) attack. In response to infection, TIRs can produce a cyclic adenosine diphosphate-ribose (ADPR) signaling molecule, which activates an effector that depletes the host of the essential metabolite NAD+ to limit phage propagation. How bacterial TIRs recognize phage infection is not known. Here we describe the sensing mechanism for the staphylococcal Thoeris defense system, which consists of two TIR domain sensors, ThsB1 and ThsB2, and the effector ThsA. We show that the major capsid protein of phage Φ80α forms a complex with ThsB1 and ThsB2, which is sufficient for the synthesis of 1''-3' glycocyclic ADPR (gcADPR) and subsequent activation of NAD+ cleavage by ThsA. Consistent with this, phages that escape Thoeris immunity harbor mutations in the capsid that prevent complex formation. We show that capsid proteins from staphylococcal Siphoviridae belonging to the capsid serogroup B, but not A, are recognized by ThsB1/B2, a result that suggests that capsid recognition by Sau-Thoeris and other anti-phage defense systems may be an important evolutionary force behind the structural diversity of prokaryotic viruses. More broadly, since mammalian toll-like receptors harboring TIR domains can also recognize viral structural components to produce an inflammatory response against infection, our findings reveal a conserved mechanism for the activation of innate antiviral defense pathways.

INTRODUCTION

Numerous bacterial innate immune systems exhibit structural and/or functional homology with those observed in plants and animals (Wein and Sorek, 2022). In metazoans, the immune response begins with the recognition of pathogen-associated molecular patterns (PAMPs) by pattern recognition receptors such as the membrane-embedded Toll-like receptors (TLRs), leading in some cases to the synthesis of cyclic nucleotide second messengers that activate downstream effector responses (Burroughs et al., 2015; Doron et al., 2018; Li and Wu, 2021; Medzhitov et al., 1997). The Thoeris immune system of prokaryotes shares fundamental characteristics with TLR immune pathways, featuring proteins with toll/interleukin-1 receptor (TIR) domains capable of generating cyclic nucleotides that activate effector proteins to prevent viral (phage) propagation (Doron *et al.*, 2018; Ka et al., 2020; Ledvina and Whiteley, 2024; Tamulaitiene et al., 2024). Present across nine distinct taxonomic phyla and found in approximately 4% of the bacterial and archaeal genomes examined, Thoeris systems are significantly represented in microbial defense mechanisms and can be classified into two different types depending on their genetic composition (Ofir et al., 2021). Type I Thoeris systems are comprised of a phage infection sensor with a TIR domain (ThsB) and an effector with a STALD (Sir2/TIR-Associating LOG-Smf/DprA) NAD-binding domain (ThsA). Upon viral infection, ThsB initiates the production of an nicotinamide adenine dinucleotide (NAD)-derived cyclic nucleotide, glycocyclic ADP-ribose (gcADPR) (Leavitt et al., 2022; Manik et al., 2022; Ofir *et al.*, 2021), which binds to the STALD domain of ThsA and induces a conformational change that activates NAD+ degradation by the Sir2 domain (Ofir *et al.*, 2021; Tamulaitiene *et al.*, 2024). NAD+ depletion arrests

the growth of the infected cells and prevents viral propagation, providing community-level immunity through the replication of the uninfected cells within the population (Ka *et al.*, 2020).

How ThsB senses phage invasion to activate the type I Thoeris response remains unknown. Here we investigate this unanswered question in the bacterium *Staphylococcus aureus*. We demonstrate that the major head protein (Mhp), the most abundant component of viral capsids, from different staphylococcal phages directly interacts with ThsB TIR proteins to stimulate the synthesis of gcADPR and initiate the Thoeris immune response.

RESULTS

Thoeris provides anti-phage protection in staphylococci

A search for Thoeris systems in *S. aureus* revealed 32 unique but highly conserved operons (Supplementary Data File 1). We decided to investigate how the type I Thoeris system present in *S. aureus* 08BA02176 (Golding et al., 2012), hereafter designated Sau-Thoeris, senses phage infection to activate immunity. The Sau-Thoeris operon carries three genes (Fig. 1A) encoding two TIR-containing proteins, called ThsB1 and ThsB2, which produce a gcADPR signaling molecule (Leavitt *et al.*, 2022; Ledvina and Whiteley, 2024; Ofir *et al.*, 2021; Tamulaitiene *et al.*, 2024), and a gcADPR-dependent effector, called ThsA, which was recently demonstrated to limit phage propagation by degrading NAD+ (Ofir *et al.*, 2021; Tamulaitiene *et al.*, 2024). To study this system, we cloned the full Sau-Thoeris operon (*thsA/B1/B2*), as well as different combinations of *ths*

genes that we used as controls, into the staphylococcal vector pE194 (Horinouchi and Weisblum, 1982b) under the control of the P*spac* IPTG-inducible promoter for expression in the laboratory strain *Staphylococcus aureus* RN4220 (Kaltwasser et al., 2002). We tested immunity against seven different staphylococcal phages and found that expression of *thsA/B1/B2*, but not of *thsB1* or *thsB2* alone, reduced viral propagation, measured as plaque formation on top agar plates, of Φ80α-vir (Banh et al., 2023), ΦNM1γ6 (Goldberg et al., 2014), ΦNM4γ4 (Heler et al., 2015), ΦJ1, ΦJ2, and ΦJ4 (Banh *et al.*, 2023), but not Φ12γ3 (Modell et al., 2017) (Fig. 1B). Similar results were obtained after infection of an *S. aureus* RN4220 strain carrying the Sau-Thoeris operon under the control of its native promoter in the chromosome (Fig. S1A). Consistent with previous reports (Ofir *et al.*, 2021), Sau-Thoeris immunity depended on the multiplicity of infection (MOI) and provided full defense of a bacterial culture at low phage concentrations (MOI 0.1 and 1; Figs. 1C and S1B), measured as the optical density at 600 nm (OD_{600}) of the culture after infection. In addition, Sau-Thoeris immunity can be activated after the induction of a Φ80α prophage with the DNA-damaging agent mitomycin C (MMC), resulting in the growth of the bacterial culture (Fig. 1D) and in a significant decrease in the production of viable viral particles, measured as plaque-forming units (PFU) (Fig. 1E). We also measured activation of the Sau-Thoeris response using a colorimetric assay to quantify the depletion of oxidized and reduced NAD (NAD+ and NADH, respectively) in cell lysates upon induction of the Φ80α prophage, an experiment that resulted in a significant decrease in NAD detection after MMC treatment, only in the presence of the full *ths* operon (Fig. 1F). Finally, we used fluorescence microscopy to visualize Sau-Thoeris defense at the cellular level. We

incubated staphylococci with a modified Φ80α-vir phage that expresses GFP (Φ80α-vir^{GFP}) (Banh *et al.*, 2023) in order to identify the infected cells. Green fluorescence decreased in staphylococci expressing ThsA/B1/B2, without cell lysis. In contrast, in cells harboring only the sensor genes *thsB1/B2*, GFP accumulation was followed by bacterial lysis (Fig. 1G). Altogether, these data show that, as previously reported for other species (Doron *et al.*, 2018; Ofir *et al.*, 2021), Sau-Thoeris activation results in a depletion of NAD+ levels that inhibits viral propagation.

The phage major head protein activates Thoeris *in vivo*

After establishing a system to study Thoeris immunity in staphylococci, we set out to investigate how this response is triggered during phage infection. To do this we isolated Φ80α-vir phages that could form plaques in the presence of Sau-Thoeris, with the expectation that they would carry mutations in genes that are required for the activation of immunity. Since we were unable to observe discrete plaques after a single round of Φ80α-vir infection (Fig. 1B), we performed five sequential infections through the inoculation of supernatants of infected cultures into fresh staphylococci carrying Sau-Thoeris. We obtained individual plaques after this process, and we selected four to isolate the escaper phages and sequence their genomes (Supplementary Sequences 1). In all cases we detected the same mutation in *gp47*, the gene encoding Φ80α-vir's major head protein (hereafter abbreviated Mhp for all the phages used in this study), which generated a missense amino acid substitution, V273A. To corroborate the role of this mutation in the evasion of Sau-Thoeris response, we infected liquid cultures with Φ80α-vir(*mhp*^{V273A}). Addition of the mutant phage resulted in complete lysis in the presence of ThsA/B1/B2, and immunity was restored when staphylococci carried a

second plasmid that expressed wild-type Mhp (Fig. 2A). Preparations of the escaper phage displayed the same plaquing efficiency and plaque size as wild-type Φ80α-vir in the absence of immunity (Fig. S2A). In the presence of Sau-Thoeris Φ80α-vir(*mhp*^{V273A}) was able to form plaques, but at a lower efficiency than in the absence of defense. The viability of the escaper phage indicates that the V273A substitution does not prevent capsid formation and therefore it is possible that the mutation eludes immunity as part of a fully formed viral procapsid. To determine whether other proteins that are involved in capsid formation are required for the development of a proper Sau-Thoeris response, and to expand our results to a different staphylococcal virus, we performed deletions of the genes involved in capsid formation in the temperate phage ΦNM1 (Fig. S2B), through genetic engineering of prophages integrated in the genome of *S. aureus* RN4220. Capsid assembly in ΦNM1 begins with the formation of an empty precursor called the procapsid, comprised of 415 units of the major head protein (encoded by *gp43*) that directly associate with 100-200 units of a scaffolding protein (*gp42*), a 12-unit portal protein complex (*gp39*), which together with the terminase subunits is responsible for packaging the phage DNA into the capsid in an ATP-dependent manner (Quiles-Puchalt et al., 2014), and approximately 20 units of a minor head protein (*gp40*), whose role in capsid biogenesis is not clear (Spilman et al., 2011). This region (Fig. S2C) also harbors a small open reading frame of unknown function present, *gp41*. We knocked out these genes as well as *rinA*, required for the transcription of the phage structural genes (Ferrer et al., 2011), and complemented each deletion strain with plasmids expressing the missing gene, cloned on the staphylococcal plasmid pC194 (Horinouchi and Weisblum, 1982a) under the control of the IPTG-inducible P*spac* promoter

(Kaltwasser *et al.*, 2002). We induced lysogenic cultures with MMC and spotted the supernatants on lawns of staphylococci carrying an empty vector or a rescue plasmid (Fig. S2C). Except for *gp41*, we detected plaques only in the presence of the complementing vector, a result that corroborated both the essentiality of the disrupted genes as well as the identity of each mutant prophage. To test Sau-Thoeris activation, we induced the mutant prophages in the presence of *thsB1/B2* or *thsA/B1/B2* and measured NAD depletion (Fig. 2B). We found that, compared to a wild-type prophage control, induction of Δ*rinA* and Δ*gp43* mutants failed to reduce the levels of NAD within lysogens. Complementation of the Δ*gp43* lysogen with iis corresponding complementing plasmid (pMhp) restored NAD+ depletion after MMC treatment (Fig. 2C). Since absence of the portal, minor head or scaffolding proteins prevents the formation of the procapsid structure, these results demonstrate that the major head protein itself, and not a fully mature capsid, is necessary for the activation of the Sau-Thoeris response.

To test if Mhp is also sufficient to trigger Sau-Thoeris immunity, we introduced pMhp into non-lysogenic *S. aureus* RN4220 carrying a second plasmid harboring different versions of the *ths* operon to achieve expression of the major head protein of ΦNM1 in the absence of phage infection. We measured NAD levels and found that only in the presence of the full *ths* operon, but not *thsB1/B2* alone, expression of Mhp significantly reduced the concentration of NAD within staphylococci (Fig. 2D). In contrast, introduction of the V273A escaper mutation into ΦNM1's Mhp abrogated NAD depletion (Fig. 2D). Since NAD deficiency should inhibit the growth of staphylococci, which we observed during the microscopy analysis of infected hosts (Fig. 1G), we hypothesized that expression of wild-type, but not the V273A mutant, Mhp in the absence of phage

infection should prevent the replication of staphylococci. Indeed, enumeration of colony-forming units (CFU) after addition of IPTG showed a significant decrease of viable cells in the presence of the full Thoeris operon when compared to the induction of cultures expressing only ThsB1/B2. In contrast IPTG induction of Mhp^{V273A} expression did not affect colony formation, showing a similar CFU count to that of cultures not expressing Mhp (Fig. 2E). In addition, growth of the cultures was also inhibited by over-expression of wild-type, but not V273A, Mhp (Fig. 2F). Altogether these results demonstrate that the major head protein of staphylococcal phages ΦNM1 and Φ80α is necessary and sufficient for the activation of the Sau-Thoeris response.

ThsB1/B2 form a complex with the major head protein *in vivo*

To determine whether the Mhp interacts directly with the Thoeris sensors, ThsB1 and ThsB2, during the phage lytic cycle, we constructed a plasmid that expressed both a hexahistidyl-tagged (His_6) ThsB1 and 3xFLAG-tagged (FLAG) ThsB2, or the reverse, under the control of an IPTG-inducible promoter and introduced these constructs into *S. aureus* RN4220::ΦNM1 lysogens. We first confirmed that the addition of the tags to ThsB1 or ThsB2 did not impact function *in vivo* (Extended Data Fig. 3A). Following overexpression of tagged ThsB1 and ThsB2, we induced the prophage with MMC, and used a cobalt resin to separate the hexahistidyl-tagged ThsB1 or ThsB2. Western blot of the pulled-down proteins using anti-FLAG antibody showed the formation of a stable complex between ThsB1 and ThsB2 only when ΦNM1's lytic cycle was induced, which depended on the presence of *gp43* (Fig. 3A). Importantly, SDS-PAGE of the pulled-down samples revealed the presence of a third protein that copurified with the ThsB1/B2 complex (Fig. 3B). Mass spectrometry analysis of the gel area containing this

193 protein identified it as Mhp (Supplementary Data File 2 and Fig. S3B). We also
194 investigated the effect of the Mhp V273A mutation on the formation of the ThsB1/B2
195 complex. To do this we performed pull-down experiments in staphylococci harboring
196 pMhp plasmids for the over-expression of wild-type and V273A mutant Mhp, in the
197 absence of phage infection. Similarly to the results obtained during induction of the
198 ΦNM1 prophage, SDS-PAGE of the proteins copurified with hexa-histidyl versions of
199 ThsB1 or ThsB2, indicated the presence of a complex composed of both proteins and
200 wild-type Mhp (Fig. 3C). This tripartite complex, however, was not captured during
201 expression of Mhp^{V273A}. Instead, we observed that the mutant Mhp co-purified with
202 ThsB1, while ThsB2 did not interact with ThsB1 nor Mhp^{V273A} (Fig. 3C). This result
203 demonstrates that the V273A escaper mutation prevents the formation of the
204 ThsB1/B2/Mhp complex.

205 Finally, we determined whether the isolated complexes were catalytically active. First,
206 the complex purified after prophage induction (Figs. 3A-B) was incubated with NAD+ to
207 test their cyclase activity (Fig. S3C) using high-performance liquid chromatography
208 (HPLC) to detect the generation of gcADPR. To be able to interpret the resulting
209 chromatograms, we determined the retention times for NAD+ and both possible cyclic
210 products, 1''-2-gcADPR and 1''-3-gcADPR (Fig. S3D). We found that the complex
211 pulled-down by His_6-ThsB1 or ThsB2-His_6 produced 1"-3'-gcADPR only when the wild-
212 type prophage was induced; not in the absence of a prophage or during induction of
213 ΦNM1(Δ*gp43*) (Fig. 3D-E). To test for the full Sau-Thoeris response, we determined
214 whether 1"-3'-gcADPR produced by the ThsB1/B2/Mhp complex can activate ThsA to
215 cleave NAD+ into nicotinamide (NAM) and ADPR (Fig. S3E). The complexes pulled-

down by His_6-ThsB1 in the presence of ThsB2-FLAG and wild-type or V273A mutant major head protein (Fig. 3C) were incubated with NAD+ and purified His_6-ThsA. After establishing the retention times of the cleavage products (Fig. S3D; note that NAM absorbance at 250 nm is much lower than that of the other compounds used in this study), we found that the complex enriched in the presence of wild-type Mhp, but not Mhp^{V273A}, were able to stimulate ThsA to produce NAM and ADPR (Fig. 3F). Based on these results, we conclude that Sau-Thoeris immunity is initiated by the interaction between viral Mhp, ThsB1 and ThsB2, a tripartite complex that cannot form during infection with escaper phages expressing Mhp^{V273A}.

ThsB1 interacts with Mhp to recruit ThsB2 and stimulate its cyclase activity

The presence of two ThsB subunits, both essential for immunity (Fig. 1E), is an intriguing feature of the Sau-Thoeris system; their individual functions and how they coordinate them for the synthesis of gcADPR during phage infection is not known. The results presented in Figure 3C demonstrated that ThsB1 and ThsB2 do not interact with each other in the absence of Mhp. In addition, the experiment suggested a possible scenario in which, during infection, the interaction between Mhp and ThsB1 recruits ThsB2 to generate an active complex capable of catalyzing the cyclization of NAD into gcADPR, and that the V273A mutation prevents ThsB2 recruitment. We tested this model by expressing hexa-histidyl-tagged versions of ThsB1 or ThsB2 alone, not as a pair, infecting the cultures with Φ80α-vir (MOI 10) for 20 minutes and capturing each sensor protein using cobalt affinity chromatography. SDS-PAGE of the purified proteins showed that Mhp co-purifies with ThsB1, but not ThsB2 (Fig. 4A), a result that supports our model of Mhp activation.

Next, we investigated which subunit performs the cyclase reaction. To do this, we generated AlphaFold structures for ThsB1 (Fig. S4A) and ThsB2 (Fig. S4B) and aligned them to closely related and previously characterized TIR proteins *Bacillus cereus* ThsB (BcThsB; PDB: 6LHY), *Acinetobacter baumannii* TIR domain (AbTir; PDB: 7UXU), human sterile alpha and TIR motif containing preotein 1 (SARM1; PDB: 6O0R) and *Arabidopsis thaliana* resistance protein RPP1 (PDB: 7DFV) (Fig. S4C). This comparison revealed a conserved active site featuring the catalytic glutamate located across a phenylalanine residue (which in other related proteins could be either an alanine or a tyrosine) (Shi et al., 2024), and enabled us to identify the putative active sites for ThsB1 (containing E318 and F242; Fig. S4C) and ThsB2 (containing E81 and F6; Fig. S4C). We made double substitutions of glutamate for glutamine and phenylalanine for alanine in both proteins and found that the ThsB2 mutations (E81Q and F6A), but not the ThsB1 mutations (E318Q and F242A), disrupted immunity against Φ80α-vir in a plaquing assay (Fig. 4B). These results suggest that the catalytic activity of ThsB2 is required for the synthesis of the second messenger. To test this, we expressed ThsB2^{F6A}-His$_6$ along with ThsB1 and ThsA, and performed pulldown experiments using lysates of staphylococci infected with Φ80α-vir at an MOI 10, collected 20 minutes post-infection. We found that the F6A mutation does not interfere with the formation of the complex with ThsB1 and Mhp (Fig. 4C). We then tested the isolated complex for cyclase activity *in vitro*. As opposed to the complex isolated after pull-down of wild-type ThsB2-His$_6$, we were unable to detect the generation of gcADPR, even in the presence of a wild-type ThsB1 (Fig. 4D). Altogether, these results support a model in which, upon phage

infection, viral Mhp and ThsB1 interact to recruit ThsB2 and stimulate its NAD+ cyclase activity.

Sau-Thoeris senses the hexameric form of Mhp

The structure of Mhp from Φ80α [Mhp(Φ80α)] has been solved experimentally (Fig. S5A) and demonstrated to be a hexamer (Dearborn et al., 2017) (Fig. S5B). Importantly, oligomeric complexes of the major head protein can form in the absence of other structural components of the procapsid (Spilman *et al.*, 2011). We used AlphaFold3 to explore possible interactions between this structure and ThsB1 and ThsB2. Supporting the results showing co-purification between Mhp and ThsB1, but not ThsB2 (Fig. 4A), the predicted structure showed that ThsB1 forms a dimer that bridges Mhp to the ThsB2 cyclase, directly interacting with the center of the Mhp hexameric ring on one side, and with two ThsB2 monomers on the other (Fig. 4E). In this AlphaFold3 model, V273 is located in the perimeter of the ring and does not make a direct contact with ThsB1 (Fig. 4E, inset), a prediction consistent with the experimental result showing that the V273A escape mutation does not prevent the interaction of ThsB1 and Mhp (Fig. 3C). In addition, the structural model of the mutant hexamer differs from that formed by wild-type Mhp (Fig. S5C; root mean square deviation of atomic positions (RMSD) values 10.698 Å, 12,922 atoms). Therefore, the combination of the different AlphaFold3 predictions with the available escaper mutant experimental data altogether suggest that ThsB1 senses the hexameric complex formed by Mhp.

The Mhp complex is held together through the interaction of two loops, the 12-residue P-loop and the 30-residue E-loop, located approximately 60 Å apart at opposite ends of the monomer (Johnson and Chiu, 2007; Spilman *et al.*, 2011) (Fig. S5A). E- and P-

loops from different monomers associate with each other to form the hexameric ring of Mhp (inset, Fig. S5B). V273 is situated within the P-loop and therefore we believe that the mutation to alanine could affect the interaction with the E-loop to generate an altered hexameric conformation (Fig. S5C). We wondered whether mutations in the E-loop could result in similar structural variations of the capsid complex that would prevent the activation of the ThsB1/B2 complex. We used the ConSurf database (Ben Chorin et al., 2020) to look for conserved residues within the E-loop, which allowed us to identify a tryptophan residue in position 84, which is highly conserved but substituted by a lysine in some sequences. We speculated that the mutation W84K would be tolerated and lead to the formation of a functional capsid that, given the divergent chemical properties of these two amino acids, could display an altered conformation, and possibly escape ThsB1 recognition. We first checked that the mutation did not disrupt capsid formation. We induced a ΦNM1(Δ*gp43*) lysogen harboring an empty vector control or a plasmid expressing either wild-type Mhp, Mhp^{V273A} or Mhp^{W84K} from an IPTG-inducible promoter. After induction of the defective prophage with MMC, Mhp^{W84K} enabled the formation of as many PFUs as both wild-type and V273A mutant capsid proteins (Fig. S5D). We also engineered this mutation into Φ80α-vir and found that it enabled similar levels of escape from Sau-Thoeris immunity as the V273A mutation (Fig. S2C). We then assessed whether over-expression of Mhp^{W84K} from a plasmid was sufficient to activate the Sau-Thoeris response, and found that the mutant Mhp was unable to mediate the reduction of NAD+ levels observed after over-expression of the wild-type capsid protein (Fig. 2D). Similarly to the AlphaFold3 model of hexameric Mhp^{V273A}, the prediction for the Mhp^{W84K} mutant showed alterations in the capsid complex that could explain the inability to

stimulate ThsB1/B2 cyclase activity (Fig. S5E; RMSD=11.970 Å, 13,233 atoms). We then performed pull-downs of His_6-ThsB1 or ThsB2-His_6 in the presence of FLAG-tagged ThsB2 or ThsB1, respectively, after over-expression of Mhp^{W84K}, and found that the mutant capsid protein did not interact with either ThsB1 or ThsB2 (Fig. 3C). This result demonstrated that the W84K substitution prevents the formation of the Mhp/ThsB1/ThsB2 complex even in the presence of an intact P-loop. Given that V273 and W84 are far apart in the Mhp monomer but located closely in the hexameric form of this protein, the finding that mutations in either of these residues prevents Sau-Thoeris activation strongly suggests that the association between capsid proteins, and not the Mhp monomer, is required for the sensing of phage infection by ThsB1/B2.

Viral major head protein is sufficient to stimulate ThsB1/B2 cyclase activity *in vitro*

Given that the experiments described above involved the pull-down of proteins from full cell extracts, they cannot rule out whether other cell components not detected by SDS-PAGE, in addition to Mhp, are necessary for the stimulation of ThsB1/B2 cyclase activity. Therefore, we investigated the minimal requirements for ThsB1/B2 activation by performing biochemical reactions with purified proteins and analyzing the reaction products using HPLC. We obtained pure preparations of His_6-ThsA, His_6-ThsB1, and ThsB2-His_6 through affinity chromatography of staphylococcal cell lysates over-expressing the tagged proteins using cobalt resin (Fig. 5A). Because Mhp did not tolerate the addition of affinity tags, we used a method previously developed (Spilman *et al.*, 2011) to purify Mhp and the V273A mutant, from lysates of *S. aureus* RN4220 over-expressing these proteins (harboring pMhp plasmids, see above), using PEG

330 precipitation followed by separation in a sucrose gradient (Fig. 5B). We first tested
331 whether His_6-ThsB1 and/or ThsB2-His_6 possess NAD+ cyclase activity (Fig. S3C) in the
332 presence of wild-type or V273A mutant Mhp. We found that wild-type Mhp only
333 stimulates the production of 1''-3' gcADPR when both ThsB proteins are present (Fig.
334 5C), but that Mhp^{V273A} was incapable of triggering the cyclase reaction (Fig. 5D). Next,
335 we corroborated the ability of purified His_6-ThsA to cleave NAD+ into ADPR and NAM
336 (Fig. S3E) (Ofir *et al.*, 2021; Tamulaitiene *et al.*, 2024) in the presence of commercially
337 available 1''-3' gcADPR (BioLog) (Fig. 5E). Finally, we recapitulated the full Sau-Thoeris
338 response *in vitro* by mixing the His_6-ThsB1 and ThsB2-His_6 sensor cyclase, the His_6-
339 ThsA effector NADase, the NAD+ substrate for both reactions, and the Mhp or Mhp^{V273A}
340 activators. We found that only the wild-type activator promoted the conversion of NAD+
341 into ADPR and NAM (Fig. 5F). Altogether, these data demonstrate that ThsB1 and
342 ThsB2 are activated by Mhp to synthesize 1''-3' gcADPR, which in turn activates ThsA.

343 **ThsB1/2 recognize conserved capsid proteins of diverse staphylococcal phages**

344 The above results demonstrated that the Mhp from the staphylococcal phages Φ80α-vir
345 and ΦNM1γ6 interact with ThsB1 to activate the Sau-Thoeris response. Our initial
346 experiments indicated that this system also provides immunity against ΦNM4γ4, ΦJ1,
347 ΦJ2, ΦJ4, but not Φ12γ3 (Fig. 1B). Therefore, we hypothesized that ThsB1/B2 would
348 recognize the major head protein of these phages, except for that of Φ12γ3, to trigger
349 the Sau-Thoeris response. To investigate whether the sequence and/or structure of
350 Mhp(Φ12γ3) is fundamentally different than that of the Mhps derived from the rest of the
351 phages tested in this study, we performed a multiple sequence alignment to generate
352 the phylogenetic tree of the six Mhps, using the ΦNM1γ6 homolog as the reference

353 sequence. Indeed, we found that Mhp(Φ12γ3) is the most distant member of this group
354 of structural proteins (Fig. S6A). Sequence divergence was reflected in a marked
355 structural variation (based on AlphaFold3 predictions) for Mhp(Φ12γ3). We quantified
356 these differences by comparing the structure of each predicted Mhp monomer to that of
357 Mhp(ΦNM1γ6) and calculated the RMSD values. While Mhps from phages Φ80α-vir,
358 ΦNM4γ4, ΦJ1/2, ΦJ4 display a very similar folding to Mhp(ΦNM1γ6), with RMSD values
359 around 1 Å, the RMSD value of the predicted structure of Mhp(Φ12γ3) was over 27 Å
360 (Fig. S6B). The structural disparity of the Mhp(Φ12γ3) monomer is also reflected in the
361 predicted hexameric ring formed by this protein, which is notably to the hexamers
362 predicted for the rest of the Mhps investigated in this study (Fig. S6C).

363 To test whether the sequence and structural predictions correlate with the ability of the
364 different Mhps to activate the Sau-Thoeris response, we cloned the major head protein
365 gene of all these phages (ΦJ1 and ΦJ2 Mhp have the same amino acid sequence) and
366 tested their effect on different assays previously used to characterize the activating
367 properties of Φ80α and ΦNM1 Mhps. We first investigated whether overexpression of
368 Mhp was sufficient to stimulate Sau-Thoeris in the absence of infection, *in vivo*. Indeed,
369 Mhp from all phages but Φ12γ3 was sufficient to cause cell arrest in the presence of
370 ThsA/B1/B2/A, but not ThsB1/B2 alone, measured as the OD_{600} of the induced cultures
371 (Fig 6A and Fig. S6D), as well NAD+ depletion (Fig. 6B). We also purified Mhp from
372 staphylococci infected with these phages (Fig. S6E) and incubated them with purified
373 His_6-ThsB1, ThsB2-His_6 and NAD+ to test for their ability to stimulate gcADPR
374 production *in vitro.* Similarly to the *in vivo* results, we found that Mhp from ΦNM4γ4,
375 ΦJ1/2, and ΦJ4, but not Φ12γ3, activated the synthesis of 1''-3' gcADPR (Fig. 6C);

which in turn was able to induce the cleavage of NAD+ when mixed with purified His_6-ThsA (Fig. S6F). These results demonstrate that diverse staphylococcal phages have structurally conserved capsid proteins that are recognized by Sau-Thoeris to trigger defense.

DISCUSSION

Here we investigated how the *Staphylococcus aureus* Thoeris system is activated by phage during infection. We found that the expression of the major head proteins of different staphylococcal Siphoviridae phages that are susceptible to Thoeris defense mediates the association of the TIR-containing proteins ThsB1 and ThsB2. Structural predictions as well as experimental data support a model in which binding of ThsB1 to the hexameric complex formed by the capsid proteins leads to the recruitment of ThsB2 and stimulation of its cyclase activity, which converts NAD+ into the second messenger 1''-3'-gcADPR. The results that validate this mechanism of Sau-Thoeris activation are: (i) ThsB1 and ThsB2 do not interact with each other in the absence of Mhp (Fig. 3A), (ii) Mhp expression leads to its association with both ThsB1 and ThsB2 (Fig. 3B), (iii) in the absence of ThsB2, ThsB1 interacts with Mhp, but ThsB2 does not interact with Mhp in the absence of ThsB1 (Fig. 4A), and (iv) the ThsB2 putative cyclase active site is critical for the synthesis of gcADPR. An AlphaFold3 prediction for the structure of a complex formed by Mhp, ThsB1 and ThsB2 independently aligned with our experimental data, as it showed a ThsB1 dimer interacting with a hexameric Mhp capsid complex on one side of the dimer and with two individual ThsB2 subunits on the other side (Fig. 4E).

There are several features of this model that will require further investigation. For example, how ThsB1 binds the Mhp hexamer is not completely clear. Our data indicates that mutations in the P-loop (V273A) or E-loop (W84K) prevent Sau-Thoeris activation. Because these loops are 60 Å apart in the Mhp monomer but overlap in the Mhp hexamer, we conclude that ThsB1 must recognize the hexameric conformation of this phage protein (ThsB1 would have to bind across the full length of the Mhp monomer to be able to interact with both ends of the protein). However, it remains possible that ThsB1 associates with the vertex of the Mhp hexamer, where the overlapping loops that hold together the capsid complex are located, and not with the center of the ring as predicted by AlphaFold3. In this case the V273A and W84K escape mutations would directly affect ThsB1 role in Sau-Thoeris activation, instead of affecting the hexameric conformation of Mhp, as we propose. Finally, the changes experienced by ThsB2 as it goes from an inactive monomer to an active cyclase in association with ThsB1 and Mhp, remain to be determined. We believe that future structural studies of the Mhp/ThsB1/ThsB2 and Mhp/ThsB1 complexes, in the presence and absence of the NAD+ substrate, will clarify these aspects of our model.

An interesting finding from our work is that bacterial TIR proteins can cooperate to provide defense. While the best characterized Thoeris defense system, from *Bacillus spp.*, possess a single ThsB subunit, those that encode two ThsB units have been shown to employ each TIR protein to independently sense different phages (Ofir *et al.*, 2021). Although we cannot rule out the possibility that ThsB1 or ThsB2 are directly activated by phages not used in this study, our data shows, at least for the staphylococcal Siphoviridae phages we tested, an interplay between bacterial TIR

421 proteins that is somewhat reminiscent of the interaction between TIR proteins in
422 eukaryotes (Wang et al., 2006). For example, the TIR proteins TLR1 and TLR2, located
423 in the plasma membrane, interact with each other to sense ligands derived from
424 bacterial envelopes. Another example is the pairwise cooperation of TLR8 with TLR7 or
425 TLR9 within endosomal membranes to regulate the eukaryotic inflammatory response
426 upon detection of viral nucleic acids produced during infection (Wang *et al.*, 2006).

427 There are other characterized defense strategies that recognize capsid proteins as a
428 sign of infection. In *Escherichia coli*, the major capsid protein of phage SECΦ27 and
429 other related phages, directly activates the CapRel toxin-antitoxin system commonly
430 present in prophages (Zhang et al., 2022). CapRel is a single polypeptide folding into a
431 “closed” conformation in which the C-terminal domain prevents the toxic activity of the
432 N-terminal domain. Direct binding of the viral capsid protein to the inhibitory domain of
433 CapRel releases the toxic domain, triggering abortive infection immunity. Also in *E. coli*,
434 the Lit protease that causes translation inhibition during T4 infection, can be activated
435 by a peptide derived from the viral capsid protein Gp23, in the absence of phage
436 (Bergsland et al., 1990). *E. coli* CBASS systems can be activated by phage capsid
437 proteins as well. The prohead protease of phage BAS13 interacts and stimulates the
438 type I CBASS cyclase EcCdnD12 and it is sufficient to induce cells death in a CBASS-
439 dependent manner in vivo (Richmond-Buccola et al., 2024). In addition, mutations in
440 capsid-encoding genes of *Pseudomonas* and *Staphylococcus* phages have been found
441 to avoid CBASS immunity (Banh *et al.*, 2023; Huiting et al., 2023). Finally, phage T5
442 accumulates mutations in the major capsid protein precursor pb8 to evade Pycsar
443 immunity (Tal et al., 2021) and phage T7 escapes F restriction in *E. coli* through

444 mutations in major capsid protein gene 10 (Molineux et al., 1989). These findings
445 suggest an involvement of phage capsids in the activation of prokaryotic immunity. In
446 eukaryotes, TIR protein-based immunity can also be triggered by the recognition of viral
447 structural components. This is the case for TLR2, present in the surface of primary
448 human liver cells, which is activated by the adeno-associated virus capsids to induce
449 the production of inflammatory cytokines (Hosel et al., 2012). Therefore, our results
450 demonstrate a conserved mechanism for the recognition of viral structural components
451 by TIR-containing proteins to start innate immunity against infection.

452 Immunological logic dictates that bacterial defense systems sense conserved molecules
453 produced during phage infection (Gao et al., 2022; Stokar-Avihail et al., 2023).
454 Conservation of immunological targets ensures (i) that the activating molecules are
455 present in many viruses, making the immune system useful against a broad range of
456 phages, and (ii) that the target is essential for optimal phage propagation and therefore
457 difficult to mutate, reducing the chances of viral escape. We believe that the targeting of
458 Mhp by Sau-Thoeris (and of other capsid proteins by other defense systems) meets
459 both evolutionary requirements. Mhp from Φ80α is highly conserved among many
460 staphylococcal phages (Fig. S6A) and four out of five homologs were able to activate
461 Sau-Thoeris (Figs. 6 and S6D). Mhp is also essential for Φ80α propagation (Fig. S2C)
462 and we were able to find only two escape mutations, V273A and W84K, using either
463 sequential infections staphylococci carrying the Sau-Thoeris system or genetic
464 engineering based on sequence conservation, respectively. Mhp mutations that escape
465 Sau-Thoeris cannot disrupt hexamer formation, but instead result in the generation of
466 an altered hexameric conformation that cannot activate ThsB1/ThsB2 but can still

assemble into procapsids. Although such mutations are infrequent, they can accumulate as a consequence of the evolutionary arms race between phages and their prokaryotic hosts, and most likely will result in changes in capsid morphology. All the phages in this study belong to the Siphoviridae group, which can be classified into distinct serogroups based on morphological differences in their head structures (Xia and Wolz, 2014). Notably, phages Φ80α, ΦNM1, ΦNM4, ΦJ1, ΦJ2, and ΦJ4, which activate Sau-Thoeris, belong to serogroup B and have isometric capsids. In contrast, Φ12, whose Mhp avoids triggering TIR-mediated defense, belongs to serogroup A and has a more prolate head structure, lengthened in one direction (Xia and Wolz, 2014). We believe that the evasion of Sau-Thoeris immunity, and possibly other defense systems that are activated by capsid proteins, represents one important evolutionary force in the differentiation of the Φ12 capsid structure, and, more generally, in the generation of structural diversity in staphylococcal phages.

METHODS

Bacterial strains and growth conditions. The bacterial strains used in this study are listed in Supplementary Methods Table 1. *Staphylococcus aureus* strain RN4220 (Xia and Wolz, 2014) was grown at 37°C with shaking (220 RPM) in brain heart infusion (BHI) broth, supplemented with chloramphenicol (10 μg mL^{-1}) or erythromycin (10 μg mL^{-1}) to maintain pC194-based (Horinouchi and Weisblum, 1982a) or pE194-based plasmids (Horinouchi and Weisblum, 1982b), respectively. Cultures were supplemented with erythromycin (5 μg mL^{-1}) to select for strains with chromosomally integrated Sau-*Thoeris* or Sau-*thsB1/B2*. Gene expression was induced by the addition of 1 mM isopropyl-d-1-thiogalactopyranoside (IPTG), where appropriate.

Bacteriophage propagation. The bacteriophages used in this study are listed in Supplementary Methods Table 2. To generate a high titer phage stock, an overnight culture of *S. aureus* RN4220 was diluted 1:100 and outgrown to mid-log phase (~90 min) in BHI broth supplemented with 5 mM $CaCl_2$. The culture was diluted to an optical density measurement at 600 nm (OD_{600}) of 0.5 (~$1x10^8$ CFU mL^{-1}). The culture was infected by adding phage at a multiplicity of infection (MOI) of 0.1 (~$1x10^7$ PFU mL^{-1}), or by inoculating with either a single picked plaque or scrape of a frozen stock. The infected culture was grown at 37°C with shaking and monitored for lysis (full loss of turbidity was typically observed ~3-4 hr). Culture lysates were centrifugated (4,300 x g for 10 min) to pellet cellular debris. The supernatant was collected, passed through a sterile membrane filter (0.45 μm), and stored at 4°C. Phage concentrations were determined by serially diluting the obtained stock in 10-fold increments and spotting 2.5 μL of each dilution on BHI soft agar mixed with RN4220 and supplemented with 5 mM $CaCl_2$. After incubation overnight at 37°C, individual plaques (i.e. zones of no bacterial growth) were counted, and the viral titer was calculated.

Molecular cloning. The plasmids (and details of their construction) and the oligonucleotide primers used in this study are listed in Supplementary Methods Table 3 and Supplementary Methods Table 4, respectively. The coding sequences of Sau-Thoeris and phage gene products were obtained from G blocks, genomic DNA preparations or phage stocks, respectively.

Chromosomal integration of Sau-Thoeris. Sau-Thoeris or Sau-ThsB1/B2, along with an erythromycin resistance (ermR) cassette, was integrated into the *hsdR* gene (which encodes the defective R-subunit of the restriction-modification system in *S. aureus* RN4220), an insertion site which was previously shown to not impact growth (Maguin et al., 2022). *Sau-thsA/B1/B2-ermR* and *Sau-thsB1/B2-ermR* were amplified from the plasmids pDVB223 and pCF11 respectively, using primers oCR482 and oCR483 or oCR484, which were flanked with loxP sites at both ends followed by 60-bp homology regions to *hsdR*. Electrocompetent *S. aureus* RN4220 cells harboring the recombineering plasmid pPM300 (Banh *et al.*, 2023) were electroporated with 1-2 μg of PCR product and selected for with erythromycin (5 μg mL^{-1}). Potential integrants were screened by colony PCR as well as for functional immunity, and then verified by Sanger sequencing.

Prophage recombineering. The prophage strains and the oligonucleotide primers used in this study are listed in Supplementary Methods Tables 1 and 4. A

chloramphenicol resistance (cmR) cassette flanked by loxP sites and 60 bp homology regions, were integrated within codons for phage genes of interest corresponding to the homology overhangs. The loxP CmR was amplified from a G-block (Azenta), using primers oCR24 and oCR25, oCR26 and oCR37, oCR30 and oCR31, oCR32 and oCR33, oCR485 and oCR486, oCR487 and oCR488, oCR489 and oCR490, oCR491 and oCR492, oCR493 and oCR494, oCR495 and oCR496, which were all flanked with 60-bp homology regions. Electrocompetent *S. aureus* RN4220 cells harboring the recombineering plasmid pPM300 were electroporated with 1-2 μg of PCR product and selected for with chloramphenicol (5 μg mL^{-1}). Potential integrants were screened by colony PCR as well as for functional immunity, and then verified by Sanger sequencing.

Generation of Φ80α-vir(*mhp*^{W84K}). Wild-type Φ80α-vir was passaged on a liquid culture of *S. aureus* RN4220 harboring a plasmid (pCR186) encoding the *mhp*^{W84K} gene flanked by 500-nt upstream and downstream homology arms corresponding to Φ80α *gp46* and *gp48*, respectively. To isolate individual plaques, the lysed culture supernatant spotted onto a lawn of RN4220 harboring a type II-A Sau CRISPR-Cas targeting plasmid (pCR187) in BHI soft agar for counter-selection against wild-type phage and enrichment of Φ80α-vir::*mhp*^{W84K}. The mutation was confirmed by Sanger sequencing.

Soft-agar phage infection. 100 μL of an overnight bacterial culture was mixed with 5 mL BHI soft agar supplemented with 5 mM $CaCl_2$ and poured onto BHI agar plates to solidify at room temperature (~15 min). Phage lysates were serially diluted 10-fold and 2.5 μL was spotted onto the soft agar surface. Once dry, plates were incubated at 37°C overnight and visualized the next day. Individual plaques (zones of no bacterial growth) were enumerated manually.

Liquid culture phage infection. Overnight cultures were diluted 1:100 in BHI supplemented with 5 mM $CaCl_2$ and the appropriate antibiotic for selection, outgrown at 37°C with shaking to mid-log phase (~90 min), and normalized to OD_{600} 0.5. For the desired MOI, a calculated volume of phage stock was added to each culture and 150 μL was seeded into each well of a 96-well plate. OD_{600} was measured every 10 min in a microplate reader (TECAN Infinite 200 PRO) at 37°C with shaking.

Protein expression and purification. ThsA, ThsB1, and ThsB2 were expressed and purified using the following approach: transformed *S. aureus* RN4220 were grown in BHI broth with 1 mM IPTG at 37°C with shaking to OD_{600} 1, at which point the culture was cooled on ice for 10 min and bacteria were harvested. Pellets were resuspended in lysis buffer (25 mM Tris pH 7.4, 100 mM NaCl, 10% glycerol, 2 mM β-mercaptoethanol, 5 mM $MgSO_4$), and subjected to a single freeze-thaw cycle. The cells were incubated at 37°C with Lysostaphin, DNase I, and EDTA-free protease inhibitor cocktail for 30 min. After incubating, the cells were lysed using sonication (70% amplitude, 10 sec on/off, 2 min total). Lysates were clarified by centrifugation and applied to cobalt affinity resin. After binding, the resin was washed extensively with high salt lysis buffer (500 mM) prior to elution with lysis buffer containing 200 mM imidazole. Eluted proteins were subjected to overnight 4°C dialysis into reaction buffer (25 mM Tris pH 7.4, 100 mM NaCl, 10% glycerol, 2 mM β-mercaptoethanol). The next day, proteins were concentrated using

10,000 MWCO centrifugal filters (Amicon). Purified proteins were visualized by SDS-PAGE and used for downstream *in vitro* assays.

Purification of native major head proteins. Native major head proteins from Φ80α, ΦNM1, ΦNM4, ΦJ1, ΦJ2, ΦJ4, and Φ12 were expressed and purified either according to an established protocol (Johnson and Chiu, 2007; Spilman *et al.*, 2011) using *S. aureus* cells harboring pMhp or as follows: PEG-precipitated phage particles were resuspended in unfolding buffer (4M guanidine-HCL, 50 mM Tris-HCl pH 8.0, and 150 mM NaCl). Proteins were then layered on a 10-40% sucrose gradient and separated by centrifugation at 100,000g for 2 hours. The gradients were manually fractionated from the top and each fraction was analyzed by SDS-PAGE. Fractions with capsid protein were subjected to dialysis into refolding buffer (25 mM Tris pH 7.4, 100 mM NaCl, 10% glycerol, 2 mM β-mercaptoethanol, 5 mM $MgSO_4$) overnight at 4°C. The final precipitate was removed by centrifugation and the supernatant was used for downstream enzymatic assays.

Nucleotide synthesis assays. Nucleotide synthesis assays were performed using a variation of the method described by (Ka *et al.*, 2020). The final reactions (25 mM Tris pH 7.4, 100 mM NaCl, 10% glycerol, 2 mM β-mercaptoethanol, 100 μM NAD+, 1 uM head protein, and 1 µM enzyme) were started with the addition of enzyme. All reactions were incubated for 2 hours at 37°C. To isolate the gcADPR product for HPLC analysis, nucleotide synthesis reaction conditions were scaled up to 200 μL reactions. Reactions were incubated with gentle shaking for 2 hr at 37°C. Following incubation, reactions were filtered through a 3,000 MWCO centrifugal filter (Amicon) to remove protein and immediately used for HPLC analysis.

ThsA NADase assay. NADase assays were performed with a 1:20 dilution of crude ThsB product or 100 nM purified 1''-3' gcADPR diluted into final reactions (25 mM Tris pH 7.4, 100 mM NaCl, 10% glycerol, 2 mM β-mercaptoethanol, 100 μM NAD+ and 1 µM enzyme) and were started with the addition of enzyme. All reactions were incubated for 2 hours at 37°C. To isolate the degradation products for HPLC analysis, nucleotide synthesis reaction conditions were scaled up to 200 μL reactions. Reactions were incubated with gentle shaking for 2 hr at 37°C. Following incubation, reactions were filtered through a 3,000 MWCO centrifugal filter (Amicon) to remove protein and immediately used for HPLC analysis.

NAD+ colorimetric assay. Detection of NAD from cell lysates was performed using an NAD/NADH colorimetric assay kit (Abcam, ab65348). To generate lysates for analysis, an overnight culture of *S. aureus* RN4220 with partial or full Thoeris was diluted 1:100 and outgrown to mid-log phase (~90 min) in BHI broth supplemented with 5 mM $CaCl_2$. The culture was diluted to OD_{600} of 0.3. The culture was either infected by adding phage at MOI 1, or a prophage was induced with the addition of 1 μg/ml MMC. The infected or induced cultures were grown at 37°C with shaking for 1-2 hrs. Pelleted cells were resuspended in 1X PBS with lysostaphin. After incubating cells at 37°C for 45 min, the resulting lysate was used for analysis and processed according to the manufacturers protocol.

Nucleotide HPLC Analysis. Reaction products were analyzed using the 1460 HPLC system (Agilent) with a diode array detector at 260 nm. Sample (10 μl) was loaded onto

a C18 column (100 x 2.0 mm, S-3 μm, 12 nm; YMC) equilibrated in 60 mM KH_2PO_4, 40 mM K_2HPO_4 buffer. Separation was performed at a flow rate of 1.2 mL min^{-1} using a gradient program for mobile phase (acetonitrile): 0-10 min.

Structural prediction and analysis. The amino acid sequences of Thoeris proteins or Φ80α-vir, ΦNM1, ΦNM4, ΦJ1, ΦJ2, ΦJ4, and Φ12 Major Heads were used to seed a position-specific iterative BLAST (PSI-BLAST) search of the NCBI non-redundant protein and conserved domain databases (composition-based adjustment, E-value threshold 0.01). A structure for all major head proteins was predicted using AlphaFold3 as a monomer or hexamer. Following structure determination, pairwise structural comparison of the rank 0 models was performed using PyMol. All predicted structures were compared to the solved structure of the Φ80α prohead (PDB: 6B0X). The ConSurf database was used to visualize and pinpoint conserved structural and functional features of the major heads.

Time-lapse fluorescence microscopy. *S. aureus* cells harboring incomplete (*thsB1/B2*) or full (*thsA/B1/B2*) Sau-Thoeris were loaded onto microfluidic chambers using the CellASIC ONIX2 microfluidic system. After cells became trapped in the chamber, they were supplied with BHI medium with 5 mM $CaCl_2$ under a constant flow of 5 μl h^{-1}. After 1 hr, GFP-tagged Φ80α-vir was flowed through the chambers for 1 hr, before switching back to growth medium. Phase contrast images were captured at 1,000x magnification every 2 min using a Nikon Ti2e inverted microscope equipped with a Hamamatsu Orca-Fusion SCMOS camera and the temperature-controlled enclosure set to 37°C. GFP was imaged using a GFP filter set using an Excelitas Xylis LED Illuminator set to 2% power, with an exposure time of 100 ms. Images were aligned and processed using the NIS Elements software.

Generation and isolation of escaper bacteriophages. Overnight cultures of *S. aureus* RN4220 were diluted 1:100 and outgrown at 37°C with shaking for 1 hr, infected with Φ80α-vir (MOI 1) for 20 min. Cultures were allowed to lyse for 3 hr before pelleting debris and sterile-filtering the supernatant to obtain phage. 100 μL of RN4220 overnight cultures harboring Sau-Thoeris were infected with a high titer mutant phage library in BHI soft agar and then plated. All plaques were collected and the soft-agar infection was repeated five times. After the fifth passage at 37°C overnight, individual phage plaques were picked from the top agar and resuspended in 50 μL of BHI liquid medium. Phage lysates were further purified over two rounds of passaging on RN4220 harboring Sau-Thoeris. Genomic DNA from high titer phage stocks was extracted using previously described methods (Jakociune and Moodley, 2018) and was submitted to SeqCenter for whole genome sequencing and assembly.

Cobalt enrichment of ThsB complex. His-tagged ThsB1 or ThsB2 were each expressed with the complementary 3xFLAG-tagged ThsB. After expression of the ThsB proteins with 1 mM IPTG, cells were either infected with Φ80α-vir (MOI 10) for 20 min or ΦNM1 prophage was induced by the addition of 1 μg/mL mitomycin C for 1 hr 30 min. Where indicated, the ThsB proteins were co-expressed with Mhp from a plasmid. The resulting cells were collected by centrifugation and resuspended in 25 mM Tris pH 7.4, 100 mM NaCl, 10% glycerol, 2 mM β-mercaptoethanol, 5 mM $MgSO_4$ with lysostaphin, DNase1 and EDTA-free protease inhibitor cocktail. The cells were lysed at 37°C with

shaking for 30 min before brief sonication. Lysates were clarified by ultracentrifugation and applied to cobalt affinity resin (~0.2 mg). After binding, the resin was washed six-ten times with lysis buffer prior to elution with lysis buffer containing 200 mM imidazole. Eluted proteins were visualized by SDS-PAGE and western blot using anti-His6 and anti-3xFLAG antibodies.

Phylogenetic analysis of Thoeris from *S. aureus*. Bioinformatically predicted Thoeris systems in S. aureus were identified in Doron et al., 2018 (Doron *et al.*, 2018). Unique Thoeris systems were identified by analyzing the protein sequences of these predicted systems in Geneious Prime 2024.0.5.

Statistical analysis. All statistical analyses were performed using GraphPad Prism v9.5.1. Error bars and number of replicates for each experiment are defined in the figure legends. Comparisons between groups for viral titer, gene expression, colony-forming units, and NAD+ concentration were analyzed by unpaired parametric t-test, two-tailed with no corrections.

Acknowledgements. We would like to thank the members of the Marraffini laboratory for constructive feedback and encouragement. LAM is an investigator of the Howard Hughes Medical Institute. CBF is supported by the National Science Foundation Graduate Research Fellowship under Grant 1946429. DVB is supported by an NIH Ruth L. Kirschstein NRSA F30 Individual Predoctoral Fellowship (F30AI157535) and an NIH Medical Scientist Training Program grant (T32GM152349) to the Weill Cornell/Rockefeller/Sloan Kettering Tri-Institutional MD-PhD Program. We would also like to thank the Rockefeller University Proteomics core for their assistance with mass spectrometry.

Author contributions. Project was conceived by CGR. Experiments were designed by CGR, CBF, DVB, and LAM. DVB performed cloning and initial testing of the Sau-Thoeris system. CGR and CBF conducted and analyzed all other experiments. The paper was written by CGR, CBF, and LAM, with input from DVB.

Competing interests: LAM is a cofounder and Scientific Advisory Board member of Intellia Therapeutics and Ancilia Biosciences, and a co-founder of Eligo Biosciences.

Data availability: Source data are provided with this paper. Any additional data from this study are available from the lead contact upon request.

REFERENCES

Banh, D.V., Roberts, C.G., Morales-Amador, A., Berryhill, B.A., Chaudhry, W., Levin, B.R., Brady, S.F., and Marraffini, L.A. (2023). Bacterial cGAS senses a viral RNA to initiate immunity. Nature *623*, 1001-1008.

Ben Chorin, A., Masrati, G., Kessel, A., Narunsky, A., Sprinzak, J., Lahav, S., Ashkenazy, H., and Ben-Tal, N. (2020). ConSurf-DB: An accessible repository for the evolutionary conservation patterns of the majority of PDB proteins. Protein Sci. *29*, 258-267.

Bergsland, K.J., Kao, C., Yu, Y.T., Gulati, R., and Snyder, L. (1990). A site in the T4 bacteriophage major head protein gene that can promote the inhibition of all translation in Escherichia coli. J. Mol. Biol. *213*, 477-494.

Burroughs, A.M., Zhang, D., Schaffer, D.E., Iyer, L.M., and Aravind, L. (2015). Comparative genomic analyses reveal a vast, novel network of nucleotide-centric systems in biological conflicts, immunity and signaling. Nucleic Acids Res. *43*, 10633-10654.

Dearborn, A.D., Wall, E.A., Kizziah, J.L., Klenow, L., Parker, L.K., Manning, K.A., Spilman, M.S., Spear, J.M., Christie, G.E., and Dokland, T. (2017). Competing scaffolding proteins determine capsid size during mobilization of Staphylococcus aureus pathogenicity islands. Elife *6*.

Doron, S., Melamed, S., Ofir, G., Leavitt, A., Lopatina, A., Keren, M., Amitai, G., and Sorek, R. (2018). Systematic discovery of antiphage defense systems in the microbial pangenome. Science *359*.

Ferrer, M.D., Quiles-Puchalt, N., Harwich, M.D., Tormo-Mas, M.A., Campoy, S., Barbe, J., Lasa, I., Novick, R.P., Christie, G.E., and Penades, J.R. (2011). RinA controls phage-mediated packaging and transfer of virulence genes in Gram-positive bacteria. Nucleic Acids Res. *39*, 5866-5878.

Gao, L.A., Wilkinson, M.E., Strecker, J., Makarova, K.S., Macrae, R.K., Koonin, E.V., and Zhang, F. (2022). Prokaryotic innate immunity through pattern recognition of conserved viral proteins. Science *377*, eabm4096.

Goldberg, G.W., Jiang, W., Bikard, D., and Marraffini, L.A. (2014). Conditional tolerance of temperate phages via transcription-dependent CRISPR-Cas targeting. Nature *514*, 633-637.

Golding, G.R., Bryden, L., Levett, P.N., McDonald, R.R., Wong, A., Graham, M.R., Tyler, S., Van Domselaar, G., Mabon, P., Kent, H., et al. (2012). Whole-genome sequence of livestock-associated ST398 methicillin-resistant *Staphylococcus aureus* Isolated from humans in Canada. J. Bacteriol. *194*, 6627-6628.

Heler, R., Samai, P., Modell, J.W., Weiner, C., Goldberg, G.W., Bikard, D., and Marraffini, L.A. (2015). Cas9 specifies functional viral targets during CRISPR-Cas adaptation. Nature *519*, 199-202.

Horinouchi, S., and Weisblum, B. (1982a). Nucleotide sequence and functional map of pC194, a plasmid that specifies inducible chloramphenicol resistance. J. Bacteriol. *150*, 815-825.

Horinouchi, S., and Weisblum, B. (1982b). Nucleotide sequence and functional map of pE194, a plasmid that specifies inducible resistance to macrolide, lincosamide, and streptogramin type B antibodies. J. Bacteriol. *150*, 804-814.

Hosel, M., Broxtermann, M., Janicki, H., Esser, K., Arzberger, S., Hartmann, P., Gillen, S., Kleeff, J., Stabenow, D., Odenthal, M., et al. (2012). Toll-like receptor 2-mediated innate immune response in human nonparenchymal liver cells toward adeno-associated viral vectors. Hepatology *55*, 287-297.

Huiting, E., Cao, X., Ren, J., Athukoralage, J.S., Luo, Z., Silas, S., An, N., Carion, H., Zhou, Y., Fraser, J.S., et al. (2023). Bacteriophages inhibit and evade cGAS-like immune function in bacteria. Cell *186*, 864-876.

Jakociune, D., and Moodley, A. (2018). A Rapid Bacteriophage DNA Extraction Method. Methods Protoc *1*.

Johnson, J.E., and Chiu, W. (2007). DNA packaging and delivery machines in tailed bacteriophages. Curr. Opin. Struct. Biol. *17*, 237-243.

Ka, D., Oh, H., Park, E., Kim, J.H., and Bae, E. (2020). Structural and functional evidence of bacterial antiphage protection by Thoeris defense system via NAD(+) degradation. Nat Commun *11*, 2816.

Kaltwasser, M., Wiegert, T., and Schumann, W. (2002). Construction and application of epitope- and green fluorescent protein-tagging integration vectors for *Bacillus subtilis*. Appl. Environ. Microbiol. *68*, 2624-2628.

Leavitt, A., Yirmiya, E., Amitai, G., Lu, A., Garb, J., Herbst, E., Morehouse, B.R., Hobbs, S.J., Antine, S.P., Sun, Z.J., et al. (2022). Viruses inhibit TIR gcADPR signalling to overcome bacterial defence. Nature *611*, 326-331.

Ledvina, H.E., and Whiteley, A.T. (2024). Conservation and similarity of bacterial and eukaryotic innate immunity. Nat. Rev. Microbiol.

Li, D., and Wu, M. (2021). Pattern recognition receptors in health and diseases. Signal Transduct Target Ther *6*, 291.

Maguin, P., Varble, A., Modell, J.W., and Marraffini, L.A. (2022). Cleavage of viral DNA by restriction endonucleases stimulates the type II CRISPR-Cas immune response. Mol. Cell *82*, 907-919.

Manik, M.K., Shi, Y., Li, S., Zaydman, M.A., Damaraju, N., Eastman, S., Smith, T.G., Gu, W., Masic, V., Mosaiab, T., et al. (2022). Cyclic ADP ribose isomers: Production, chemical structures, and immune signaling. Science *377*, eadc8969.

Medzhitov, R., Preston-Hurlburt, P., and Janeway, C.A., Jr. (1997). A human homologue of the Drosophila Toll protein signals activation of adaptive immunity. Nature *388*, 394-397.

764 Modell, J.W., Jiang, W., and Marraffini, L.A. (2017). CRISPR-Cas systems exploit viral
765 DNA injection to establish and maintain adaptive immunity. Nature *544*, 101-104.

766 Molineux, I.J., Schmitt, C.K., and Condreay, J.P. (1989). Mutants of bacteriophage T7
767 that escape F restriction. J. Mol. Biol. *207*, 563-574.

768 Ofir, G., Herbst, E., Baroz, M., Cohen, D., Millman, A., Doron, S., Tal, N., Malheiro,
769 D.B.A., Malitsky, S., Amitai, G., and Sorek, R. (2021). Antiviral activity of bacterial TIR
770 domains via immune signalling molecules. Nature *600*, 116-120.

771 Quiles-Puchalt, N., Carpena, N., Alonso, J.C., Novick, R.P., Marina, A., and Penades,
772 J.R. (2014). Staphylococcal pathogenicity island DNA packaging system involving cos-
773 site packaging and phage-encoded HNH endonucleases. Proc. Natl. Acad. Sci. U.S.A.
774 *111*, 6016-6021.

775 Richmond-Buccola, D., Hobbs, S.J., Garcia, J.M., Toyoda, H., Gao, J., Shao, S., Lee,
776 A.S.Y., and Kranzusch, P.J. (2024). A large-scale type I CBASS antiphage screen
777 identifies the phage prohead protease as a key determinant of immune activation and
778 evasion. Cell Host Microbe *32*, 1074-1088 e1075.

779 Shi, Y., Masic, V., Mosaiab, T., Rajaratman, P., Hartley-Tassell, L., Sorbello, M.,
780 Goulart, C.C., Vasquez, E., Mishra, B.P., Holt, S., et al. (2024). Structural
781 characterization of macro domain-containing Thoeris antiphage defense systems. Sci
782 Adv *10*, eadn3310.

783 Spilman, M.S., Dearborn, A.D., Chang, J.R., Damle, P.K., Christie, G.E., and Dokland,
784 T. (2011). A conformational switch involved in maturation of Staphylococcus aureus
785 bacteriophage 80alpha capsids. J. Mol. Biol. *405*, 863-876.

786 Stokar-Avihail, A., Fedorenko, T., Hor, J., Garb, J., Leavitt, A., Millman, A., Shulman, G.,
787 Wojtania, N., Melamed, S., Amitai, G., and Sorek, R. (2023). Discovery of phage
788 determinants that confer sensitivity to bacterial immune systems. Cell *186*, 1863-1876
789 e1816.

790 Tal, N., Morehouse, B.R., Millman, A., Stokar-Avihail, A., Avraham, C., Fedorenko, T.,
791 Yirmiya, E., Herbst, E., Brandis, A., Mehlman, T., et al. (2021). Cyclic CMP and cyclic
792 UMP mediate bacterial immunity against phages. Cell *184*, 5728-5739 e5716.

793 Tamulaitiene, G., Sabonis, D., Sasnauskas, G., Ruksenaite, A., Silanskas, A., Avraham,
794 C., Ofir, G., Sorek, R., Zaremba, M., and Siksnys, V. (2024). Activation of Thoeris
795 antiviral system via SIR2 effector filament assembly. Nature *627*, 431-436.

796 Wang, J., Shao, Y., Bennett, T.A., Shankar, R.A., Wightman, P.D., and Reddy, L.G.
797 (2006). The functional effects of physical interactions among Toll-like receptors 7, 8,
798 and 9. J. Biol. Chem. *281*, 37427-37434.

799 Wein, T., and Sorek, R. (2022). Bacterial origins of human cell-autonomous innate
800 immune mechanisms. Nat. Rev. Immunol. *22*, 629-638.

801 Xia, G., and Wolz, C. (2014). Phages of Staphylococcus aureus and their impact on
802 host evolution. Infect Genet Evol *21*, 593-601.

803 Zhang, T., Tamman, H., Coppieters 't Wallant, K., Kurata, T., LeRoux, M., Srikant, S.,
804 Brodiazhenko, T., Cepauskas, A., Talavera, A., Martens, C., et al. (2022). Direct

activation of a bacterial innate immune system by a viral capsid protein. Nature *612*, 132-140.

FIGURE LEGENDS

Figure 1. **Thoeris provides anti-phage protection in staphylococci. (A)** Schematic of the Thoeris operon present in the *Staphylococcus aureus* strain 08BA02176. The operon includes a *thsA* gene harboring a STALD domain, and two *thsB* genes, *thsB1* and *thsB2* that encode TIR domains. **(B)** Tenfold serial dilutions of different staphylococcal phages on lawns of *S. aureus* RN4220 harboring plasmids carrying either an incomplete (*thsB1/B2*) or full (*thsA/B1/B2*) Thoeris operon. **(C)** Growth of *S. aureus* RN4220 harboring plasmids carrying either an incomplete (*thsB1/B2*) or full (*thsA/B1/B2*) Thoeris operon, determined as the OD_{600} of the cultures after infection with Φ80α-vir at MOI 1. Mean of +/- S.D. of three biological replicates is reported. **(D)** Same as **(C)** but following the growth of lysogenic cultures after induction of the Φ80α prophage with MMC. **(E)** Enumeration of PFU/ml after induction of the Φ80α prophage with MMC present in lysogens harboring plasmids carrying different combinations of the *thsA*, *thsB1* and *thsB2* genes. Dotted line indicates the limit of detection. Mean of +/- S.D. of three biological replicates is reported; *p* value was obtained using an unpaired, two-tailed**,** *t*-test**. (F)** Measure of % remaining NAD+ and NADH (NAD), calculated as the ratio of the concentration of NAD+ and NADH detected in staphylococci harboring plasmids carrying different combinations of the *thsA*, *thsB1* and *thsB2* genes, to the value detected in the absence of any of the *ths* genes, after induction of the Φ80α prophage with MMC. Mean of +/- S.D. of three biological replicates is reported; *p* value was obtained using an unpaired, two-tailed**,** *t*-test**. (G)** Fluorescence microscopy of *S. aureus* RN4220 harboring plasmids carrying either an incomplete (*thsB1/B2*) or full (*thsA/B1/B2*) Thoeris operon. Images were taken every two hours after infection with Φ80α-vir-GFP phage, up to eight hours. The images are representative of three independent experiments.

Figure 2. **The phage major head protein activates Thoeris *in vivo*. (A)** Growth of *S. aureus* RN4220 harboring plasmids carrying either an incomplete (*thsB1/B2*) or full (*thsA/B1/B2*) Thoeris operon in the absence or presence of a second plasmid expressing Mhp, determined as the OD_{600} of the cultures after infection with Φ80α-vir or Φ80α-vir(*mhp*^{V273A}) at MOI 1. Mean of +/- S.D. of three biological replicates is reported. **(B)** Measure of % remaining NAD+/NADH (NAD), calculated as the ratio of the concentration of NAD+ and NADH detected in staphylococci harboring a plasmid carrying a full (*thsA/B1/B2*) Thoeris operon, to the value detected in the presence of an incomplete (*thsB1/B2*) system, after induction of the ΦNM1 prophage with MMC. Lysogens induced carried either wild-type or mutant prophages with deletions in different genes involved in capsid formation. Mean of +/- S.D. of three biological replicates is reported; *p* value was obtained using an unpaired, two-tailed**,** *t*-test**. (C)** Same as **(B)** after induction of wild-type and Δ*gp43* ΦNM1 prophages, in the presence of a plasmid that expresses Mhp. **(D)** Same as **(B)** but after IPTG induction of expression of plasmid-encoded wild-type, V273A or W84K Mhp. **(E)** Enumeration of CFU/ml after induction of the Φ80α prophage with MMC present in lysogens harboring plasmids carrying either an incomplete (*thsB1/B2*) or full (*thsA/B1/B2*) Thoeris operon. Mean of +/- S.D. of three biological replicates is reported; *p* value was obtained using an unpaired, two-tailed**,** *t*-test**. (F)** Growth of *S. aureus* RN4220 harboring plasmids carrying either an incomplete (*thsB1/B2*) or full (*thsA/B1/B2*) Thoeris operon in the presence of a second plasmid expressing either wild-type or V273A Mhp, determined as

the OD_{600} of the cultures after addition of IPTG. Mean of +/- S.D. of three biological replicates is reported.

Figure 3. **ThsB1/B2 form a complex with the major head protein *in vivo*. (A)** Immunoblot analysis of proteins extracted from staphylococci expressing hexahystidyl- (H) or FLAG- (F) tagged versions of ThsB1 or ThsB2, uninfected or infected with wild-type or Δ*gp43* ΦNM1 phage, either before (input) of after affinity chromatography using a cobalt resin. Proteins were separated by SDS-PAGE, and electrotransferred to a PVDF membrane. Tagged proteins were detected with anti- hexahystidyl (α-His) or anti-FLAG (α-FLAG) antibodies and chemiluminescence staining. **(B)** Coomassie Blue-stained SDS-PAGE of proteins isolated after cobalt resin affinity chromatography in the experiment described in **(A)**. His_6-ThsB1, 41.8 kDa; ThsB2-His_6, 23.4 kDa; Mhp, 36.8 kDa. Protein molecular weight (kDa) markers are shown. **(C)** Coomassie Blue-stained SDS-PAGE of proteins isolated from staphylococci expressing hexahystidyl- (H) or FLAG- (F) tagged versions of ThsB1 and ThsB2 and either wild-type, V273A or W84K Mhp, in the absence of phage infection, after cobalt resin affinity chromatography. Protein molecular weight (kDa) markers are shown. **(D)** HPLC analysis of the products resulting from the incubation of the proteins purified from staphylococci expressing His_6-ThsB1 and ThsB2-FLAG, uninfected or infected with wild-type or Δ*gp43* ΦNM1 phage, with NAD+, using a cobalt resin. Retention times (RT) of reactants and products are marked by dotted lines. **(E)** Same as **(D)** but using proteins extracted from staphylococci expressing ThsB1-FLAG and ThsB2-His_6. **(F)** Same as **(D)** but adding purified His_6-ThsA to the reaction.

Figure 4. ThsB1 interacts with Mhp to recruit ThsB2 and stimulate its cyclase activity. (A) Coomassie Blue-stained SDS-PAGE of proteins isolated from staphylococci expressing hexahystidyl- (H) tagged versions of ThsB1 or ThsB2, uninfected or infected with Φ80α-vir, after cobalt resin affinity chromatography. Protein molecular weight (kDa) markers are shown. **(B)** Tenfold serial dilutions of Φ80α-vir on lawns of *S. aureus* RN4220 harboring plasmids carrying either an incomplete (*thsB1/B2*) or full (*thsA/B1/B2*) Thoeris operon carrying wild-type or mutant versions of *thsB1* or *thsB2*. **(C)** Coomassie Blue-stained SDS-PAGE of proteins isolated from staphylococci expressing ThsB2, ThsB2-His_6 or $ThsB2^{F6A}$-His_6, uninfected or infected with Φ80α-vir, after cobalt resin affinity chromatography. Protein molecular weight (kDa) markers are shown. **(D)** HPLC analysis of the products resulting from the incubation of the proteins purified from staphylococci expressing ThsB2-His_6 or $ThsB2^{F6A}$-His_6, uninfected or infected with Φ80α-vir, with NAD+, using a cobalt resin. Retention times (RT) of reactants and products are marked by dotted lines. **(E)** AlphaFold3 structure of a complex formed by Φ80α Mhp (hexamer; grey) ThsB1 (two copies; yellow) and ThsB2 (two copies; teal). Two angles of the structure (90° rotation), as well as the position of residue V273 (red) are shown.

Figure 5. Viral major head protein is sufficient to stimulate ThsB1/B2 cyclase activity *in vitro*. (A) Coomassie Blue-stained SDS-PAGE of proteins purified from *E. coli* expressing His_6-ThsA (56.0 kDa), His_6-ThsB1 (41.8 kDa), and ThsB2-His_6 (23.4 kDa) using a cobalt resin. Protein molecular weight (kDa) markers are shown. **(B)** Coomassie Blue-stained SDS-PAGE of Mhp proteins, wild-type and V273A mutant (V/A) purified from staphylococci harboring pMhp plasmids, using PEG-enrichment.

Protein molecular weight (kDa) markers are shown. **(C)** HPLC analysis of the products resulting from the incubation of purified ThsB2-His_6, $ThsB2^{F6A}$-His_6 or both, with NAD+. Retention times (RT) of reactants and products are marked by dotted lines. **(D)** Same as **(C)** but after incubation of both ThsB2-His_6 and $ThsB2^{F6A}$-His_6, alone (-) or in the presence of purified wild-type or V273A mutant Mhp. **(E)** HPLC analysis of the products resulting from the incubation of purified His_6-ThsA and commercially available 1''-3' gcADPR. Retention times (RT) of reactants and products are marked by dotted lines. **(F)** Same as **(D)** but in the presence of purified His_6-ThsA.

Figure 6. ThsB1/2 recognize conserved capsid proteins of diverse staphylococcal phages. (A) Growth of *S. aureus* RN4220 harboring plasmids carrying either an incomplete (*thsB1/B2*) or full (*thsA/B1/B2*) Thoeris operon in the presence of a second plasmid expressing Mhp from different staphylococcal phages, determined as the OD_{600} of the cultures 16 hours after addition of IPTG. Mean of +/- S.D. of three biological replicates is reported; *p* value was obtained using an unpaired, two-tailed**,** *t*-test. **(B)** Measure of % remaining NAD+/NADH (NAD), calculated as the ratio of the concentration of NAD+ and NADH detected in staphylococci harboring a plasmid carrying a full (*thsA/B1/B2*) Thoeris operon, to the value detected in the presence of an incomplete (*thsB1/B2*) system, after induction of the expression of Mhp from different staphylococcal phages. Mean of +/- S.D. of three biological replicates is reported; *p* value was obtained using an unpaired, two-tailed**,** *t*-test**. (C)** HPLC analysis of the products resulting from the incubation of purified ThsB2-His_6 and $ThsB2^{F6A}$-His_6 with NAD+, in the presence of purified Mhp from different staphylococcal phages. Retention times (RT) of reactants and products are marked by dotted lines.

SUPPLEMENTARY FIGURE LEGENDS

Figure S1. Characterization of Sau-Thoeris defense. (A) Tenfold serial dilutions of Φ80α-vir on lawns of *S. aureus* RN4220 carrying either an incomplete (*thsB1/B2*) or full (*thsA/B1/B2*) Thoeris operon in a chromosomal location. **(B)** Growth of *S. aureus* RN4220 harboring plasmids carrying either an incomplete (*thsB1/B2*) or full (*thsA/B1/B2*) Thoeris operon, determined as the OD_{600} of the cultures after infection with Φ80α-vir at MOI 0, 0.1 or 10. Mean of +/- S.D. of three biological replicates is reported.

Figure S2. Major head protein is required for Sau-Thoeris activation. (A) Schematic of ΦNM1 genome, with expansion of the operon for packaging the genome and assembly of phage particles. P_E and P_L are promoters responsible for the expression of early and late viral genes, respectively. The green asterisk indicates the nonsense mutation prevents ΦNM1 lysogeny, converting it into ΦNM1γ6, a purely lytic phage. Regions of the genome involved in different stages of the viral lytic cycle are indicated. **(B)** Genes of the ΦNM1 genome required for capsid biogenesis. **(C)** Tenfold serial dilutions of Φ80a-vir phage carrying wild-type or V273A *mhp* alleles on lawns of *S. aureus* RN4220 harboring plasmids carrying either an incomplete (*thsB1/B2*) or full (*thsA/B1/B2*) Thoeris operon. **(D)** Tenfold serial dilutions of lysates obtained after MMC induction of different ΦNM1 lysogens carrying deletions on genes involved in packaging the genome and assembly of phage particles on lawns of *S. aureus* RN4220 harboring an empty vector control, or plasmids expressing the genes deleted in the prophages.

Figure S3. ThsB1-ThsB2-Mhp copurification assays. (A) Tenfold serial dilutions of Φ80a-vir phage on lawns of *S. aureus* RN4220 harboring plasmids carrying either untagged or hexahystidyl- or FLAG-tagged versions of ThsB1 or ThsB2, along with untagged ThsA. **(B)** LC-MS/MS identification of ~35 kDa protein isolated with ThsB1 and ThsB2 from infected *S. aureus* RN4220 cells shown in Figure 3B. Gel slices (n=3) were subjected to reduction, alkylation, and in-gel digestion. Peptides were extracted before being injected for LC-MS/MS analysis. Search results against the staphylococcal phage ΦNM1 proteome are presented as the percentage of sequence coverage (ΣCoverage) vs the indication of unique identified peptides (ΣPSMs). Data for the phage Mhp is shown in red. **(C)** Cyclization reaction of oxidized nicotinamide adenine dinucleotide (NAD+) mediated by the ThsB1/B2/Mhp complex, which yields 1"-3'-glyocyclic ADP-ribose (1"-3'-gcADPR) and nicotinamide (NAM). **(D)** HPLC analysis of different commercially available chemicals used in this study. **(E)** Hydrolysis reaction of oxidized nicotinamide adenine dinucleotide (NAD+) mediated by ThsA when activated by 1"-3'-gcADPR, which yields ADP-ribose (ADPR) and nicotinamide (NAM).

Figure S4. Structural analysis of ThsB1 and ThsB2. (A) Structure of ThsB1 generated by AlphaFold3, with the putative active site marked with a red square. **(B)** Same as **(A)** but for ThsB2. **(C)** Structural comparison of the predicted active sites of ThsB1 and ThisB2 (red squares in panels A and B, respectively) with the experimentally characterized active sites of different TIR proteins: *Bacillus cereus* ThsB (BcThsB; PDB: 6LHY), *Acinetobacter baumannii* TIR domain (AbTir; PDB: 7UXU), human sterile alpha and TIR motif containing preotein 1 (SARM1; PDB: 6O0R) and *Arabidopsis thaliana* resistance protein RPP1 (PDB: 7DFV).

Figure S5. Importance of Mhp hexameric form for Sau-Thoeris activation. (A) Structure Φ80α Mhp monomer (PDB: 6B0X), colored according to the different structural domains (red, N-arm; yellow, P domain and loop; green, A-domain; orange, E-loop). **(B)** Structure of the hexameric form of Φ80α major head protein (PDB: 6B0X), with one capsomer interface highlighted. The position of the residues which mutations led to immune evasion, V273 within the P-loop (tan) and W84 within the E-loop (brown), are shown. **(C)** Alphafold3 prediction of the hexameric form of Φ80α Mhp^{V273A}. **(D)** Tenfold serial dilutions of lysates obtained after MMC induction of a ΦNM1(Δ*gp43*) lysogen on lawns of *S. aureus* RN4220 harboring either an empty vector control (-), or plasmids expressing wild-type, V273A or W84K Mhp. **(E)** Sames as **(C)** but for Φ80α Mhp^{W84K}.

Figure S6. Analysis of the Sau-thoeris activating properties of Mhp from different staphylococcal phages. (A) Phylogenetic tree of the major head proteins used in this study, generated using EMBL-EBI Muscle multiple sequence alignment tool. The branch numbers indicate genetic distance from ΦNM1 Mhp calculated by the software. **(B)** Alphafold3 prediction of the monomeric form of Mhp encoded by the different phages used in this study. Structural distance is shown as the RMSD of the different Mhps compared to ΦNM1 Mhp. **(C)** Alphafold3 prediction of the hexameric form of Mhp encoded by the different phages used in this study. **(D)** Growth of *S. aureus* RN4220 harboring plasmids carrying either an incomplete (*thsB1/B2*) or full (*thsA/B1/B2*) Thoeris operon in the presence of a second plasmid expressing Mhp from different staphylococcal phages, determined as the OD_{600} of the cultures after addition of IPTG.

The values at the end of the curves, at 16 hours, were used to meke the bar graphs shown in Figure 6A. Mean of +/- S.D. of three biological replicates is reported. **(E)** Coomassie Blue-stained SDS-PAGE of Mhp proteins, purified from staphylococci harboring pMhp plasmids using PEG-enrichment. Protein molecular weight (kDa) markers are shown. **(F)** HPLC analysis of the products resulting from the incubation of purified His_6-ThsA with the products of the reactions shown in Figure 6C, obtained after mixing ThsB2-His_6, $ThsB2^{F6A}$-His_6, NAD+ purified Mhp from different staphylococcal phages. Retention times (RT) of reactants and products are marked by dotted lines.

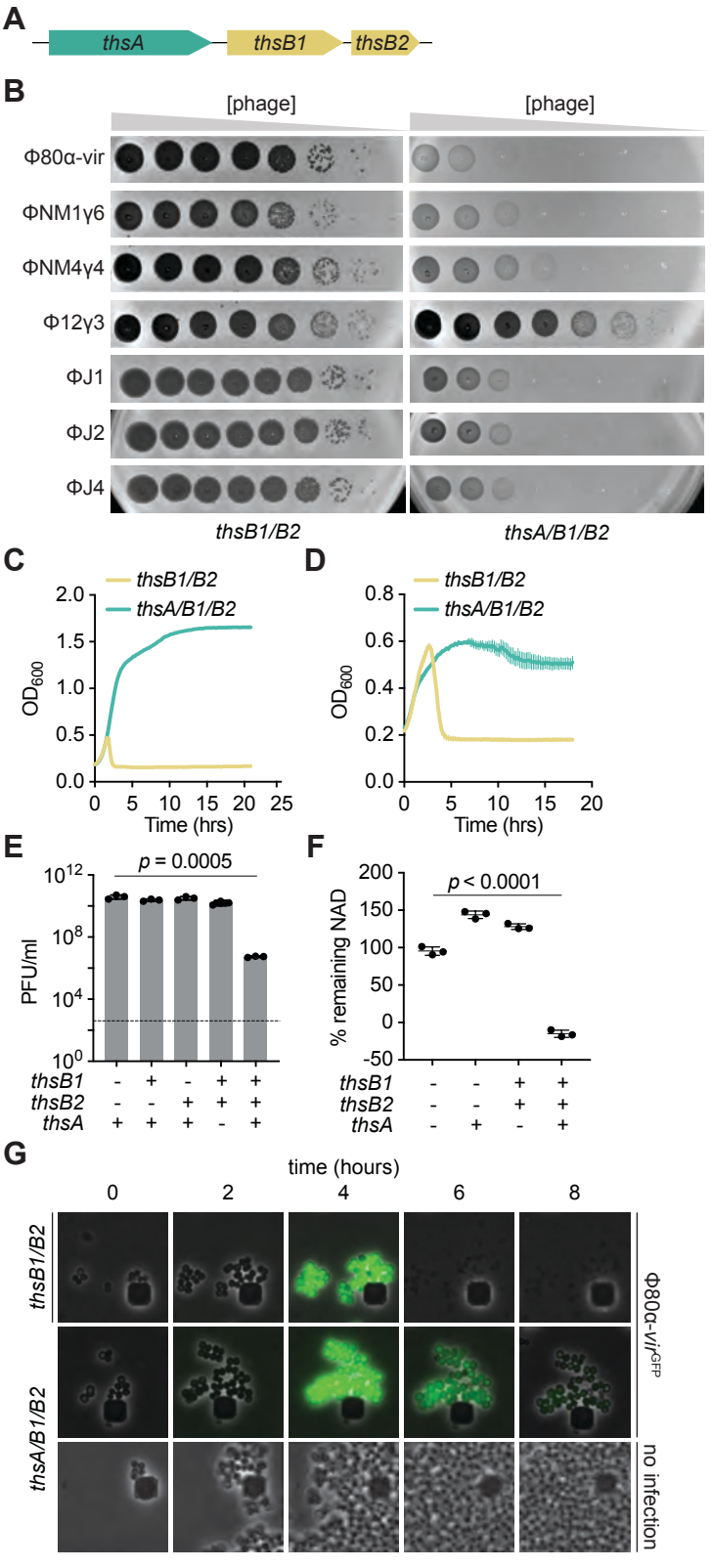

Figure 1. Roberts, Fishman *et al*.

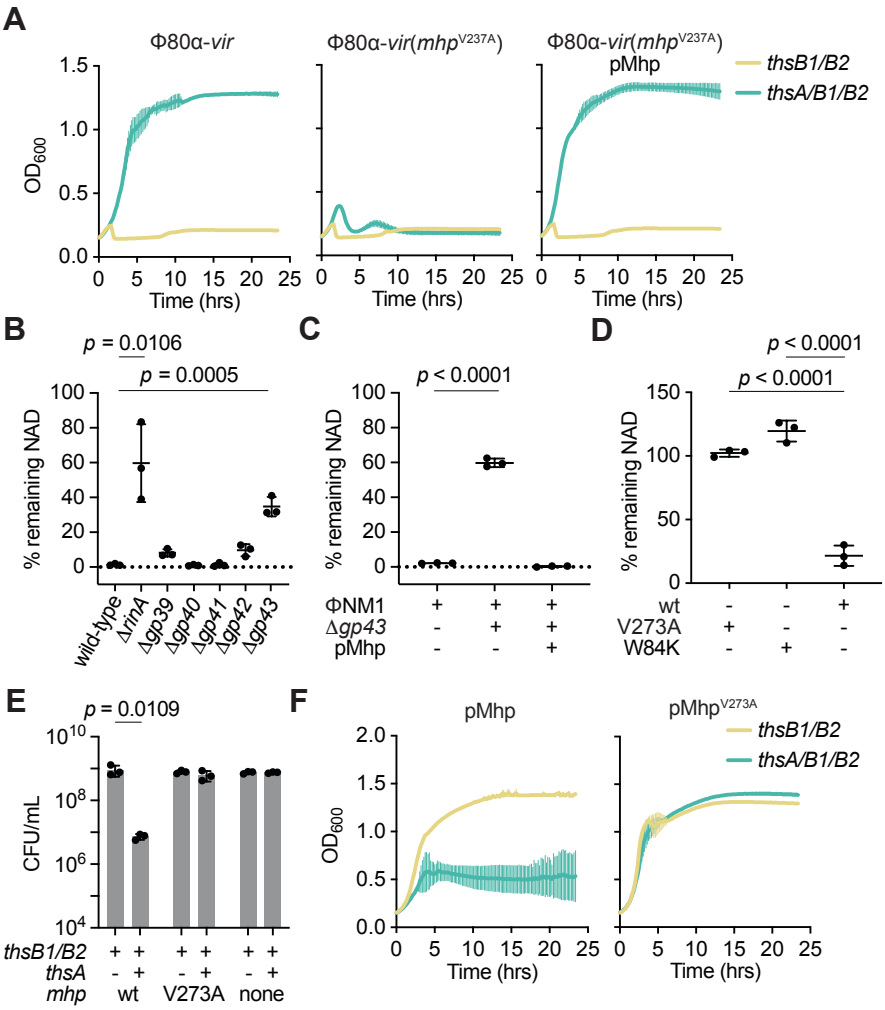

Figure 2. Roberts, Fishman *et al*.

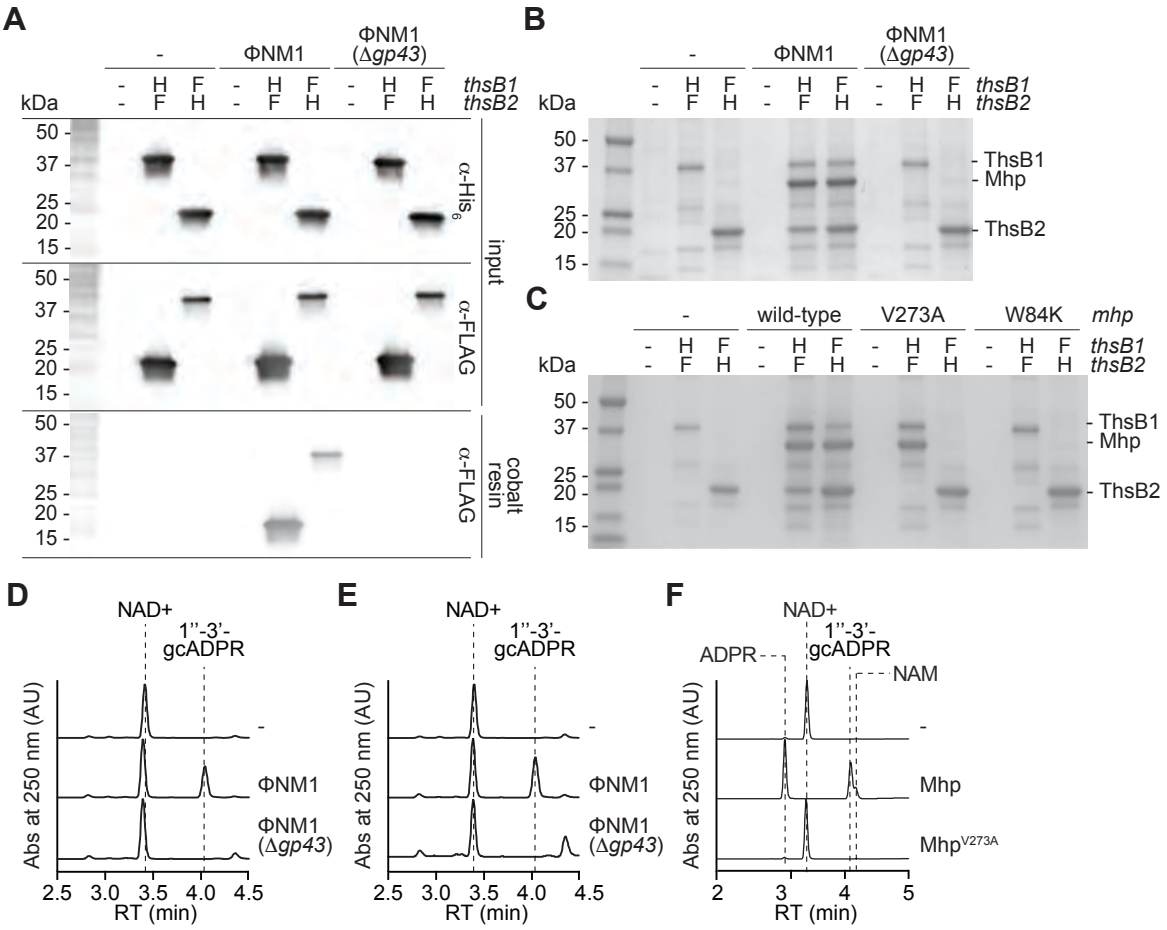

Figure 3. Roberts, Fishman *et al*.

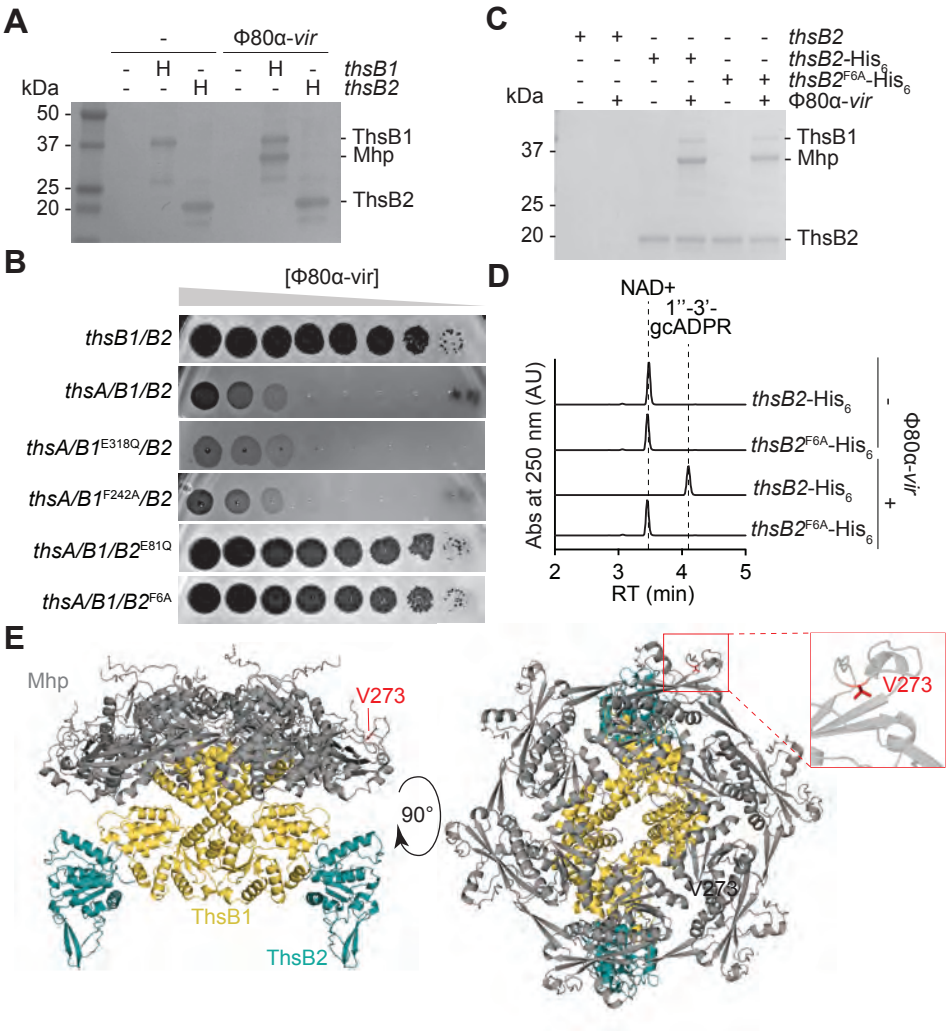

Figure 4. Roberts, Fishman *et al*.

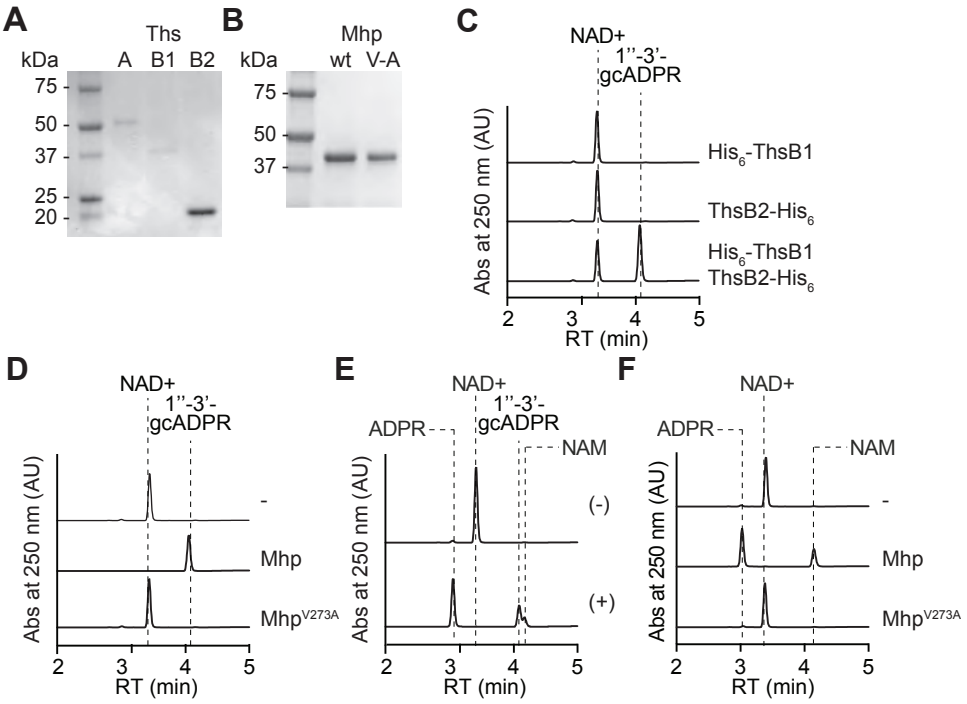

Figure 5. Roberts, Fishman, *et al*.

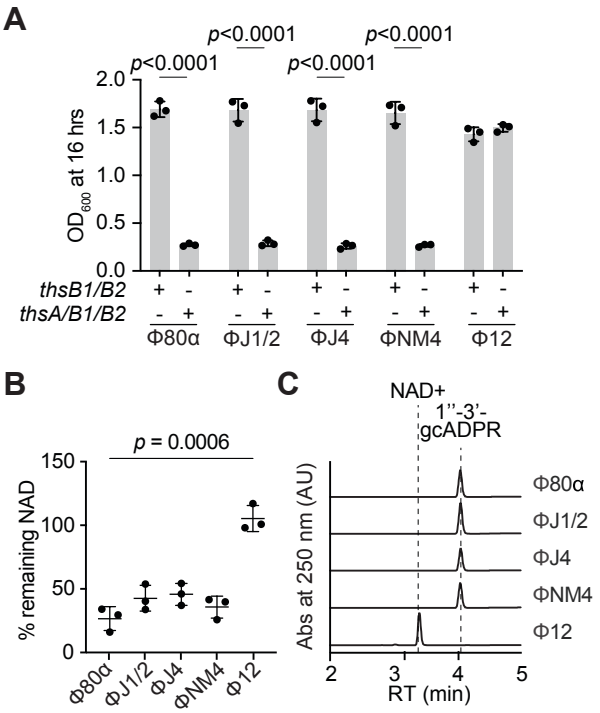

Figure 6. Roberts, Fishman, *et al*.

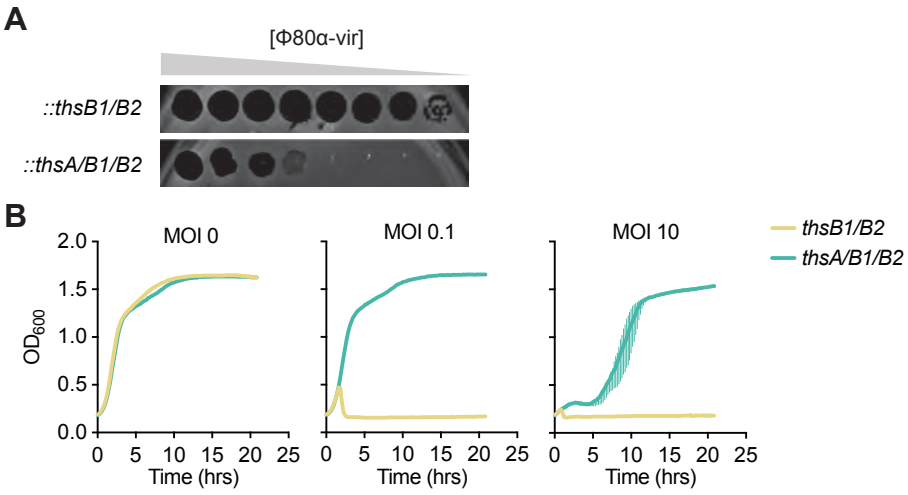

Figure S1. Roberts, Fishman *et al*.

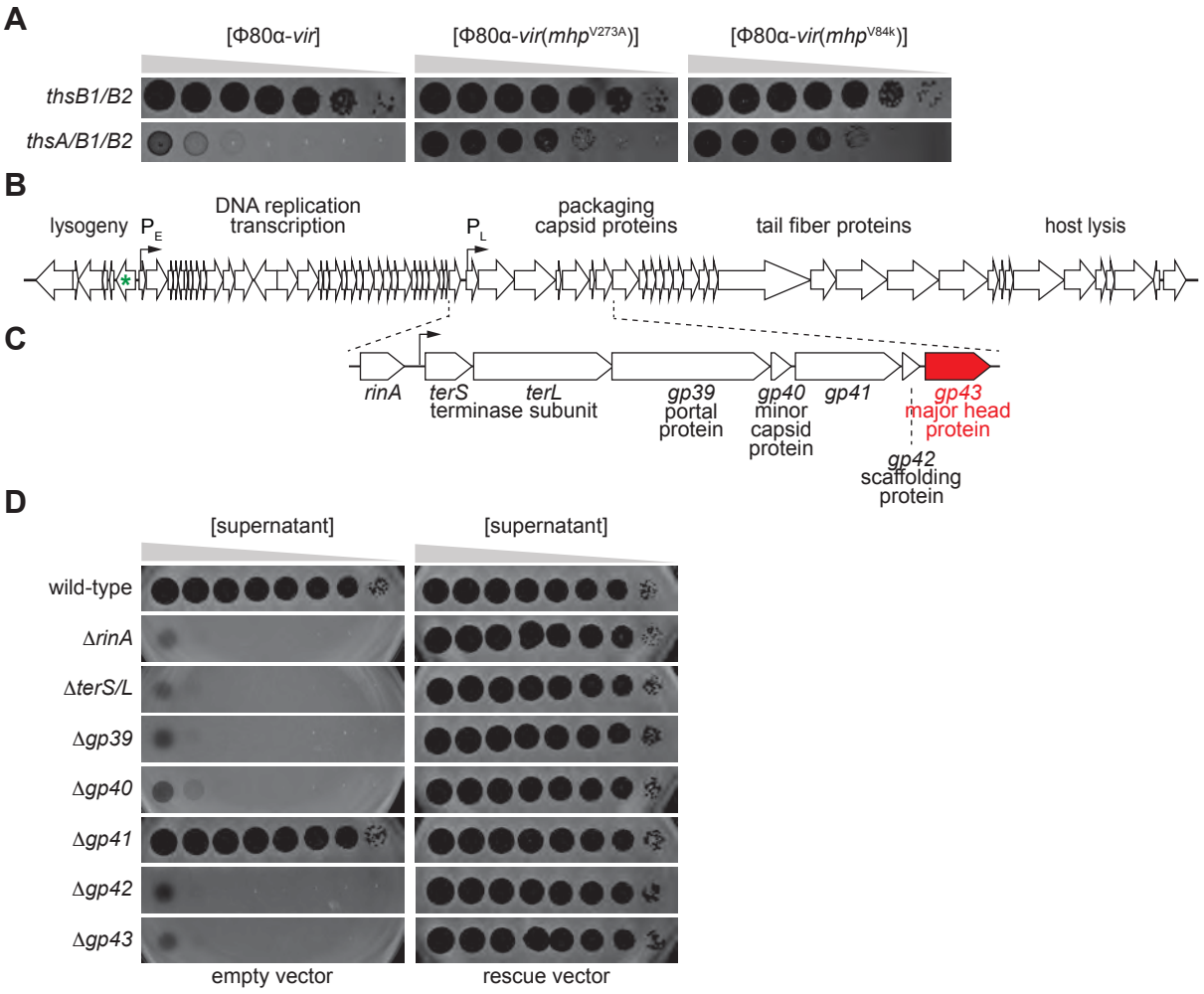

Figure S2. Roberts, Fishman *et al*.

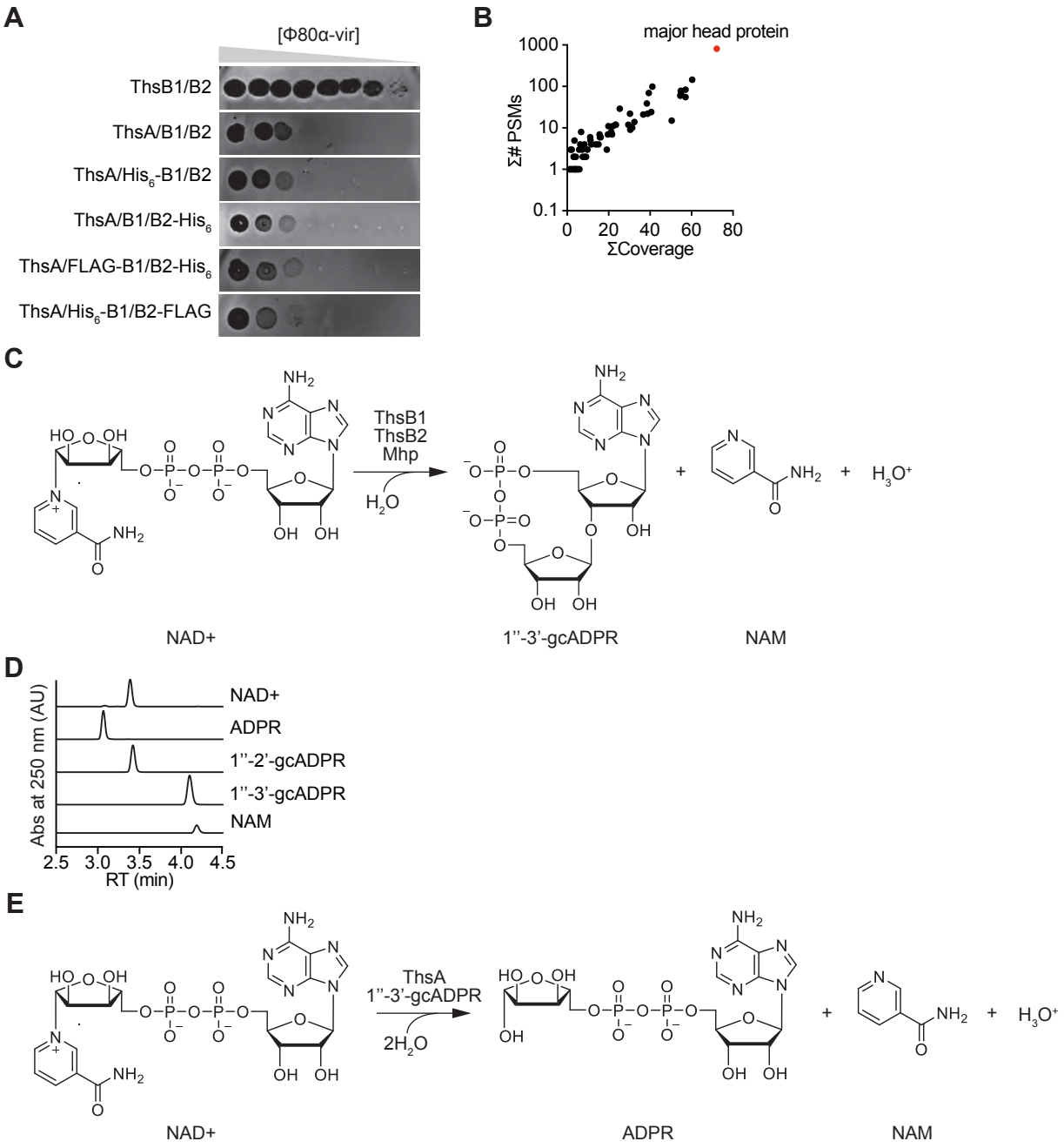

Figure S3. Roberts, Fishman *et al*.

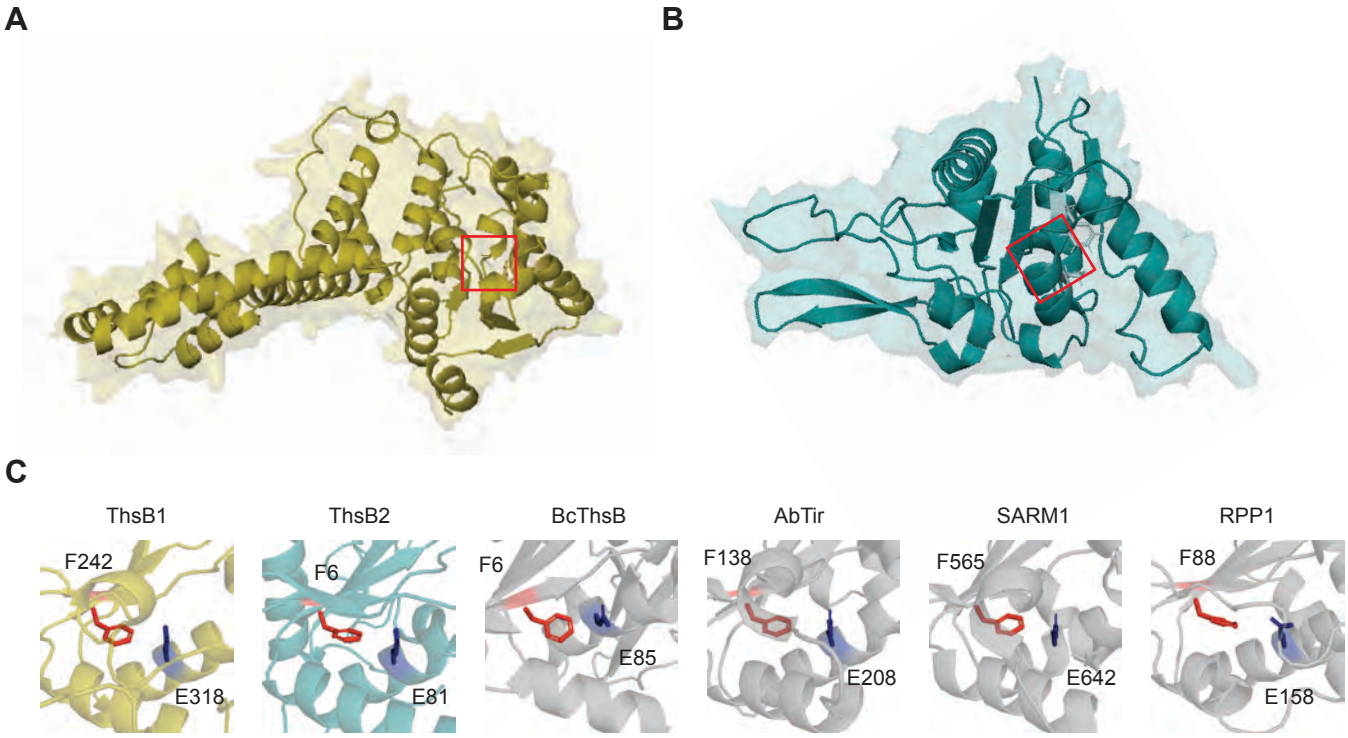

Figure S4. Roberts, Fishman *et al*.

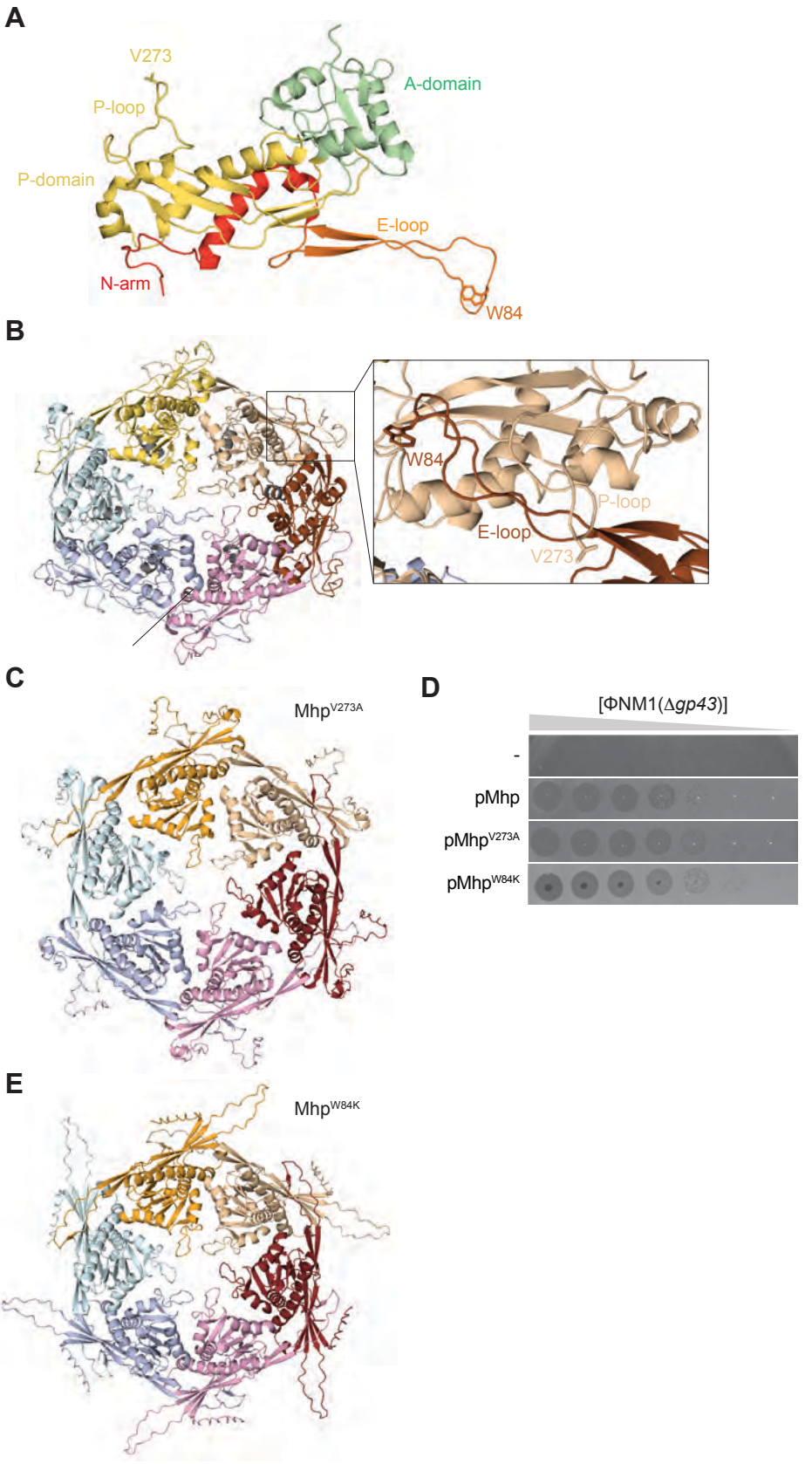

Figure S5. Roberts, Fishman *et al*.

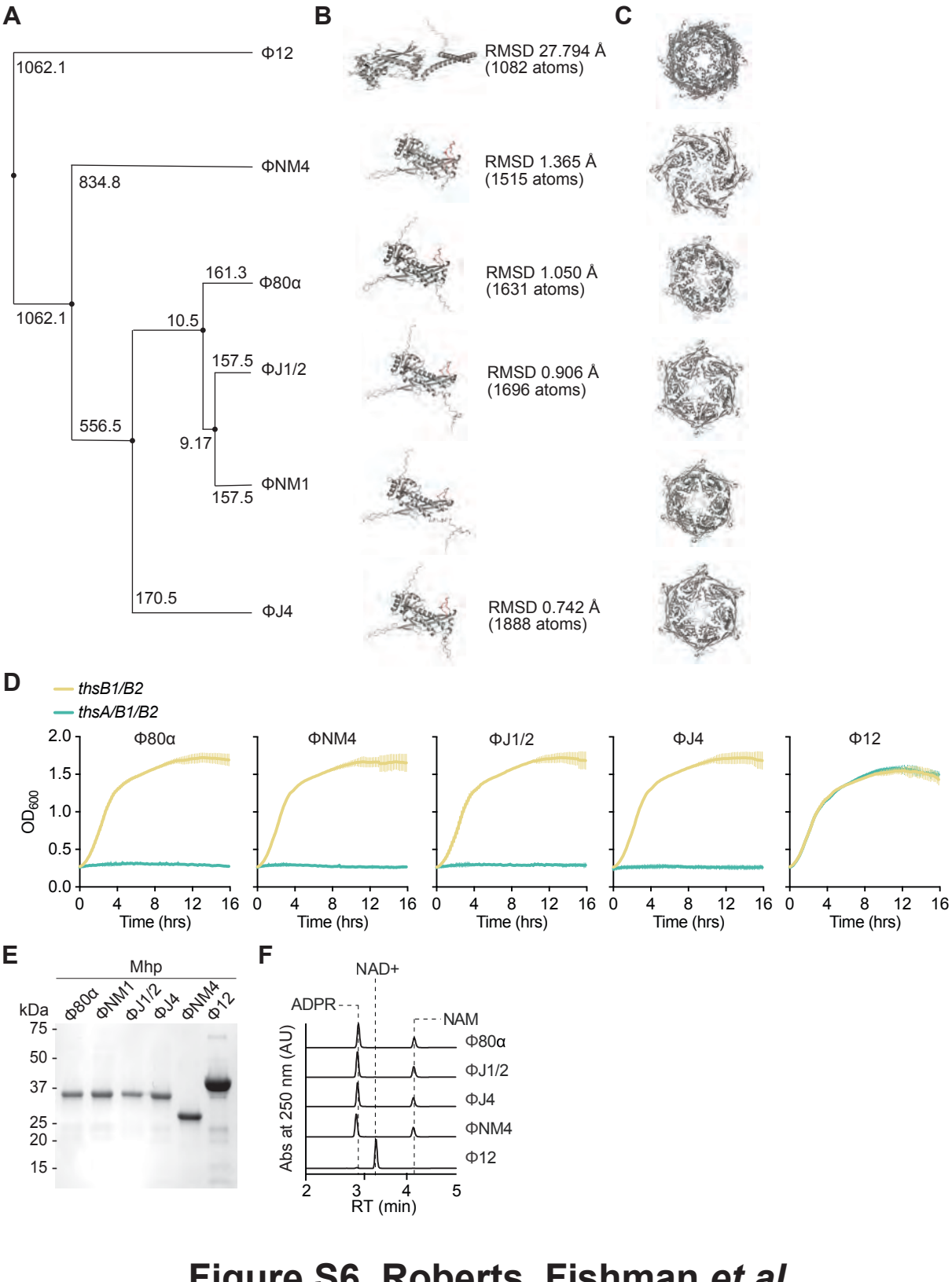

Figure S6. Roberts, Fishman *et al*.

SUPPLEMENTARY METHODS TABLES.

Supplementary Methods Table 1. Bacterial strains used in this study.

Species	Strain	Genotype	Origin
S. aureus	RN4220	Wild type	Kreiswerth et al., Nature (1983)
S. aureus	RN4220	::ΦNM1	Goldberg et al., Nature (2014)
S. aureus	RN4220	::ΦNM1ΔDnaC	Cre-loxP Recombineering (see methods)
S. aureus	RN4220	::ΦNM1ΔRinA	Cre-loxP Recombineering (see methods)
S. aureus	RN4220	::ΦNM1ΔTerS	Cre-loxP Recombineering (see methods)
S. aureus	RN4220	::ΦNM1ΔTerL	Cre-loxP Recombineering (see methods)
S. aureus	RN4220	::ΦNM1ΔPortal	Cre-loxP Recombineering (see methods)
S. aureus	RN4220	::ΦNM1ΔGp40	Cre-loxP Recombineering (see methods)
S. aureus	RN4220	::ΦNM1ΔGp41	Cre-loxP Recombineering (see methods)
S. aureus	RN4220	::ΦNM1ΔGp42	Cre-loxP Recombineering (see methods)
S. aureus	RN4220	::ΦNM1ΔMajor Head	Cre-loxP Recombineering (see methods)
S. aureus	RN4220	::Φ80α ΔMajor Head	Cre-loxP Recombineering (see methods)
S. aureus	RN4220	::Sau-Thoeris-ermR	Chromosomal integration (see methods)
S. aureus	RN4220	::Sau-ThsB1-B2-ermR	Chromosomal integration (see methods)

Supplementary Methods Table 2. Phages used in this study.

Phage	Host	Genotype	Origin
Φ80α-vir	*S. aureus*	Wild type	Banh and Roberts et al., Nature (2023)
Φ80α-vir^{GFP}	*S. aureus*	Wild type	Banh and Roberts et al., Nature (2023)
Φ80α-vir(gp47^{V273A})	*S. aureus*	Major head (gp47) V273>A (T818>C)	This study; isolated from screen for Sau-Thoeris escapers
Φ80α-vir(gp47^{W84K})	*S. aureus*	Major head (gp47) W84>K (TGG249-251>AAA)	This study; engineered by recombination using pCR186 and selected for using pCR187
ΦJ1	*S. aureus*	Wild type	Banh and Roberts et al., Nature (2023)
ΦJ2	*S. aureus*	Wild type	Banh and Roberts et al., Nature (2023)
ΦJ4	*S. aureus*	Wild type	Banh and Roberts et al., Nature (2023)
ΦNM1γ6	*S. aureus*	Wild type	Goldberg et al., Nature (2014)
ΦNM4γ4	*S. aureus*	Wild type	Heler et al., Nature (2015)
Φ12γ3	*S. aureus*	Wild type	Modell et al., Nature (2017)

Supplementary Methods Table 3. Plasmids used in this study.

Plasmid	Description	Source	Construction Notes
pPM300	Recombineering genes from phage ϕ11 under the control of an IPTG-inducible promoter and cre-recombinase under the control of an aTc-inducible promoter	Banh et al., 2023	
pDVB223	Thoeris operon from S. aureus 08BA02176, IPTG-inducible pE194-based vector for recombinant protein expression	This study	Gibson assembly: oDVB796+oDVB797 (S. aureus 08BA02176 template) oDVB_ + oDVB_ (pE194 template)
pCF8	ThsA+ThsB1, IPTG-inducible pE194-based vector for recombinant protein expression	This study	Gibson assembly: oCF.36+oCF.37 (pDVB223 template)
pCF9	ThsA+ThsB2, IPTG-inducible pE194-based vector for recombinant protein expression	This study	Gibson assembly: oCF.38+oCF.39 (pDVB223 template)
pCF10	ThsA, IPTG-inducible pE194-based vector for recombinant protein expression	This study	Gibson assembly: oCF.40+oCF.41 (pDVB223 template)
pCF11	ThsB1+ThsB2 IPTG-inducible pE194-based vector for recombinant protein expression	This study	Gibson assembly: oCF.42+oCF.43 (pDVB223 template)
pCF34	His6-ThsA+ThsB1+ThsB2, IPTG-inducible pE194-based vector for recombinant protein expression and purification of ThsA	This study	Gibson assembly: oCF.70+oCF.91 oCF.86+oCF.90 (pDVB223 template)
pCF35	ThsA+His6-ThsB1+ThsB2, IPTG-inducible pE194-based vector for recombinant protein expression and purification of ThsB1	This study	Gibson assembly: oCF.72+oCF.91 oCF.73+oCF.90 (pDVB223 template)
pCF41	gp43 (major head) from ΦNM1γ6 with escape mutation (V273A), IPTG-	This study	Gibson assembly: oCF.84+oCF.85 (pCR176 template)

	inducible pC194-based vector for recombinant protein expression		
pCF45	N315 hypothetical protein from Φ12γ3, IPTG-inducible pC194-based vector for recombinant protein expression	This study	Gibson assembly: oCF.98+oCF.99 (Φ12γ3 template) oCF.97+oCF100 (pC194 template)
pCF46	His6-N315 hypothetical protein from Φ12γ3, IPTG-inducible pC194-based vector for recombinant protein expression	This study	Gibson assembly: oCF.86+oCF.101 (pCF.45 template)
pCF47	ThsB1(F242A)+ThsB2 IPTG-inducible pE194-based vector for recombinant protein expression	This study	Gibson Assembly: oCF.102+oCF.103 (pCF.11 template)
pCF48	ThsB1(E318Q)+ThsB2 IPTG-inducible pE194-based vector for recombinant protein expression	This study	Gibson Assembly: oCF.104+oCF.105 (pCF.11 template)
pCF49	ThsB1+ThsB2(F6A) IPTG-inducible pE194-based vector for recombinant protein expression	This study	Gibson Assembly: oCF.106+oCF.107 (pCF.11 template)
pCF50	ThsB1+ThsB2(E81Q) IPTG-inducible pE194-based vector for recombinant protein expression	This study	Gibson Assembly: oCF.108+oCF.109 (pCF.11 template)
pCF51	ThsA+ThsB1+ThsB2-His6, IPTG-inducible pE194-based vector for recombinant protein expression and purification of ThsB2	This study	Gibson Assembly: oCF.110+oCF.111 (pDVB223 template)
pCF52	His6-ThsB1+ThsB2-3xFlag, IPTG-inducible pE194-based vector for recombinant protein expression and purification of ThsB1 and ThsB2	This study	Gibson Assembly: oCF.112 + oCF.114 oCF.72 + oCF.113 oCF.86 + oCF.115 (pCF.11 template)
pCF53	3xFlag-ThsB1+ThsB2-His6, IPTG-inducible pE194-based vector for recombinant protein expression and	This study	oCF.112 + oCF.117 oCF.78 + oCF.113 oCF.87 + oCF.116 (pCF.11 template)

	purification of ThsB1 and ThsB2		
pCF55	ThsA+ThsB1(F242A)+ThsB2 IPTG-inducible pE194-based vector for recombinant protein expression	This study	Gibson Assembly: oCF.102+oCF.103 (pDVB223 template)
pCF56	ThsA+ThsB1(E318Q)+ThsB2 IPTG-inducible pE194-based vector for recombinant protein expression	This study	Gibson Assembly: oCF.104+oCF.105 (pDVB223 template)
pCF57	ThsA+ThsB1+ThsB2(F6A) IPTG-inducible pE194-based vector for recombinant protein expression	This study	Gibson Assembly: oCF.106+oCF.107 (pDVB223 template)
pCF58	ThsA+ThsB1+ThsB2(E81Q) IPTG-inducible pE194-based vector for recombinant protein expression	This study	Gibson Assembly: oCF.108+oCF.109 (pDVB223 template)
pCF60	ThsB1+ThsB2 IPTG-inducible pE194-based vector for recombinant protein expression	This study	Gibson assembly: oCF.110+oCF.111 (pCF.11 template)
pCF64	Gp43(W84K) (Major Head) of ΦNM1γ6, IPTG-inducible pC194-based vector for recombinant protein expression	This study	Gibson assembly: oCF.126+oCF.127 (pCR176 template)
pCF69	His-ThsB1 IPTG-inducible pE194-based vector for recombinant protein expression	This study	Gibson Assembly: oCF.36+oCF.37 (pCF.52 template)
pCF70	ThsB2-His IPTG-inducible pE194-based vector for recombinant protein expression	This study	Gibson Assembly: oCF.136+oCF.137 (pCF.53 template)
pCF80	ThsA+His6-ThsB1+ThsB2-3xFLAG, IPTG-inducible pE194-based vector for recombinant protein expression	This study	Gibson Assembly oCF.114+oCF.115 (template pCF.35)
pCF81	ThsA+3xFLAG-ThsB1+ThsB2-His6, IPTG-inducible pE194-based vector for recombinant protein expression	This study	Gibson Assembly oCF.78+oCF.160 (template pCF.51)

pCR173	terS-Gp43 (full packaging and structure operon) of ΦNM1γ6, IPTG-inducible pC194-based vector for recombinant protein expression	This study	Gibson Assembly: oCR499+oCR500 (ΦNM1γ6 template) oCR497+oCR498 (pC194 template)
pCR174	Portal-Gp43 of ΦNM1γ6, IPTG-inducible pC194-based vector for recombinant protein expression	This study	Gibson Assembly: oCR501+oCR500 (ΦNM1γ6 template) oCR497+oCR498 (pC194 template)
pCR175	Gp40-Gp43 of ΦNM1γ6, IPTG-inducible pC194-based vector for recombinant protein expression	This study	Gibson Assembly: oCR502+oCR500 (ΦNM1γ6 template) oCR497+oCR498 (pC194 template)
pCR176	Gp43 (Major Head) of ΦNM1γ6, IPTG-inducible pC194-based vector for recombinant protein expression	This study	Gibson Assembly: oCR503+oCR500 (ΦNM1γ6 template) oCR497+oCR498 (pC194 template)
pCR177	terL (large terminase subunit) of ΦNM1γ6, IPTG-inducible pC194-based vector for recombinant protein expression	This study	Gibson Assembly: oCR504+oCR505 (ΦNM1γ6 template) oCR497+oCR498 (pC194 template)
pCR178	terS-terL of ΦNM1γ6, IPTG-inducible pC194-based vector for recombinant protein expression	This study	Gibson Assembly: oCR499+oCR505 (ΦNM1γ6 template) oCR497+oCR498 (pC194 template)
pCR179	Major Head of ΦJ1/2, IPTG-inducible pC194-based vector for recombinant protein expression	This study	Gibson Assembly: oCR497+oCR498 (pCR176 template) oCR515+oCR516 (ΦJ1/2 template)
pCR180	Major Head of ΦJ4, IPTG-inducible pC194-based vector for recombinant protein expression	This study	Gibson Assembly: oCR497+oCR498 (pCR176 template) oCR517+oCR518 (ΦJ4 template)
pCR181	Major Head of Φ80α, IPTG-inducible pC194-based	This study	Gibson Assembly: oCR497+oCR498

	vector for recombinant protein expression		(pCR176 template) oCR519+oCR520 (Φ80α template)
pCR184	Major Head of Φ80α with V273A, IPTG-inducible pC194-based vector for recombinant protein expression		Gibson assembly: oCF.84+oCF.85 (pCR181 template)
pCR185	Major Head of Φ80α with W84K, IPTG-inducible pC194-based vector for recombinant protein expression		Gibson assembly: oCF.126+oCF.127 (pCR181 template)
pCR182	Major Head of ΦNM4, IPTG-inducible pC194-based vector for recombinant protein expression	This study	Gibson Assembly: oCR497+oCR498 (pCR176 template) oCR521+oCR522 (ΦNM4 template)
pCR183	Major Head of Φ12, IPTG-inducible pC194-based vector for recombinant protein expression	This study	Gibson Assembly: oCR497+oCR498 (pCR176 template) oCR523+oCR524 (Φ12 template)
pCR186	Recombination plasmid harboring *mhp*^{W84K} gene with 500-nt upstream and downstream homology arms corresponding to Φ80α *gp46* and *gp48*, respectively	This study	Gibson Assembly: oCR589+oCR590 (pCR176 template) oCR591+oCR592 (Φ80α gDNA template) oCR593+oCR594 (pCF64 template) oCR595+oCR596 (Φ80α gDNA template)
pCR187	*S. aureus* M06/0171 type II-A CRISPR-Cas system with programmed spacer targeting wild-type Φ80α-vir	This study	Ligation of BsaI-digested pDVB47 (Banh et al., 2023) and annealed oCR597/oCR598

	but not Φ80α-vir::*mhp*^{W84K} (mutation changes PAM)		

Supplementary Methods Table 4. Oligonucleotide primers used in this study.

Primer	Sequence
oCR24	ATCAATCAAACGTTAATCCGTCTTTAAGAGATGCAACAGTCAAAAACT ACAAGCCATAACTTCGTATAGCATACATTATACGAAGTTATAGTGACA TTAG
oCR25	AGCCTTGTACGTACTCTATTGCTGTTTGTTTAGCGTGTACTTGTTTTT CATTTTGTATAACTTCGTATAATGTATGCTATACGAAGTTATTATATTT ATG
oCR26	ATACAAATATAGGCGGGGAGTTTGTACCGTCTAATACATCAAAAACA GAAATGGCAGTAACATAACTTCGTATAGCATACATTATACGAAGTTAT AGTGACATTAG
oCR27	CGTTCAATCGCACTCTTAAACTCAAGAATTTTACCTCTTCGTATACTA CAAAGATAATTAATAACTTCGTATAATGTATGCTATACGAAGTTATTAT ATTTATG
oCR59	ATCTGCTTCTATTGCTAGAGGAGAACCTCAAGAGGCTTACAGTAAGA AATATGACCATTTATAACTTCGTATAGCATACATTATACGAAGTTATAG TGACATTAG
oCR60	TGACGCTCTTCAAAAGTTGGTGTGATTGTGTAAGTAACCTCTTTTTCC ACTTCATCGTTTATAACTTCGTATAATGTATGCTATACGAAGTTATTAT ATTTATG
oCR63	TTAAGAACTGGAAGAAGAAACCAGGTAAGCCGTTAGACGTACAACTT GATGAATTAGCTGATAACTTCGTATAGCATACATTATACGAAGTTATA GTGACATTAG
oCR64	TTTATCTCTTCTGATGACACTCCTACTTGATTCGCAATACTCAATCCA AACGCCAACATGTATAACTTCGTATAATGTATGCTATACGAAGTTATT ATATTTATG
oCR95	AAATAATCATCCTCCTAAGTACAAGCTTAATTGTTATCCGCTCACAAT TCCACACATTAT
oCR96	GAGTGATCGTTAAATTTATACTGCAATCGGATGCGATTATTGAATAAA AGATATGAGAGA
oCR482	GGTGTTGAAACGCGATACTTTTCTAATAATGATAGCGAACTATTGAAG AGTCACATGTTTTATTGGAGTGTTTATGCATCCCTTAACTTACTTATTA AAT
oCR483	GCTAATTGACAAGGTCTCATAAATGACTCAGCAAACGATTGCAATGTA TTGATACGGTTATTCTGTTTATTAAAGCATTAAAACCCCATGAATTATT TT
oCR484	GCTAATTGACAAGGTCTCATAAATGACTCAGCAAACGATTGCAATGTA TTGATACGGTTATTCTGTTTATTTATTTTCTTCTACAGATATTATAATTC GTTGC
oCR485	ACGACAAAACTTAGAGTTGTTAGCAAATCGTAATCCAGCATATTACAA AATTTATGCGTTATAACTTCGTATAGCATACATTATACGAAGTTATAGT GACATTAG

oCR486	TTTATTAAACGTTTTTCATACTTAGGGAAAACCAATTTGTCTAGTGTAG CAAATTCACCTATAACTTCGTATAATGTATGCTATACGAAGTTATTATA TTTATG
oCR487	GTTACTTATTAAAGGTAATTTAAATTTAGATCCCGTAGAAGTTAGAAAA CAAAAGGAAGCATAACTTCGTATAGCATACATTATACGAAGTTATAGT GACATTAG
oCR488	CCTTCTGTTTCTCTACCTTCGCTATCAGCATAAACAGTCGGTTCTAAA AACAACACGTTAATAACTTCGTATAATGTATGCTATACGAAGTTATTAT ATTTATG
oCR489	AATAATTGCTAATGTAGTTATTAGAGGTCGACATCCTAATGAATATGT TAAAGATATGCGATAACTTCGTATAGCATACATTATACGAAGTTATAG TGACATTAG
oCR490	AATGATTTAATTGCTGCGGTCTTTTGTCGTGCTGTGCCTTCGAATTTA TTTAAGTGCTTGATAACTTCGTATAATGTATGCTATACGAAGTTATTAT ATTTATG
oCR491	TAGAGACATAGCAAGAGAGTTAAAAGGTATACGTAAAGAGTTACAAA AGCGAAACGAAACATAACTTCGTATAGCATACATTATACGAAGTTATA GTGACATTAG
oCR492	TTTTCTTTATCGGCTAATACTGCCGACCTTACGCTGTCTAAGTTTGCA TCAATAATAACTATAACTTCGTATAATGTATGCTATACGAAGTTATTAT ATTTATG
oCR493	TAAAGAAGAATTAAGTCGTCGTATGAAGCAGAAAGAAAAAGAGAAAC AAGAAGCTGTTGAATAACTTCGTATAGCATACATTATACGAAGTTATA GTGACATTAG
oCR494	TGTTCGCGTTCATATTCAGCGATTTGATCTTTGTTCATTTTTGCTAATC GTTTAGCTTCAATAACTTCGTATAATGTATGCTATACGAAGTTATTATA TTTATG
oCR495	AGGTGAAGGTCAAAAAATCGAAACATCTAAAGCTACATGGGTTAATG CTACTATGAGAGCATAACTTCGTATAGCATACATTATACGAAGTTATA GTGACATTAG
oCR496	TGTGAATAAGTGTAATTCAAAAATTCTTTTGTTACAGGTAAGATAACC CCTAATTTAAACATAACTTCGTATAATGTATGCTATACGAAGTTATTAT ATTTATG
oCR497	AAATAATCATCCTCCTAAGTACAAGCTTAA
oCR498	GACGTGGTTTAACCCGGGTAACTAGTAACT
oCR499	TTAAGCTTGTACTTAGGAGGATGATTATTTATGAACGAAAAACAAAAG AGATTCGC
oCR500	AGTTACTAGTTACCCGGGTTAAACCACGTCTTAAACTTCTCCTGGTAC TGAATCTGT
oCR501	TTAAGCTTGTACTTAGGAGGATGATTATTTATGTTAAAAGTAAACGAA TTTGAAACAGAT
oCR502	TTAAGCTTGTACTTAGGAGGATGATTATTTTTGCCTAACAAAAACACT CAAGAATATTG
oCR503	TTAAGCTTGTACTTAGGAGGATGATTATTTATGGAACAAACACAAAAA TTAAAATTAAAT

oCR504	TTAAGCTTGTACTTAGGAGGATGATTATTTATGACGAAAGTTAAATTAAACTTTAACAAA
oCR505	AGTTACTAGTTACCCGGGTTAAACCACGTCCTATAATCCTAGAGATTTTATTGTGTCAAC
oCR515	TTAAGCTTGTACTTAGGAGGATGATTATTTATGGAACAAACACAAAAATTAAAATTAAAT
oCR516	AGTTACTAGTTACCCGGGTTAAACCACGTCTTAAACTTCTCCTGGTACTGAATC
oCR517	TTAAGCTTGTACTTAGGAGGATGATTATTTATGGAACAAACACAAAAATTAAAATTAAAT
oCR518	AGTTACTAGTTACCCGGGTTAAACCACGTCTTAAACTTCTCCTGGAACTGAAG
oCR519	TTAAGCTTGTACTTAGGAGGATGATTATTTATGGAACAAACACAAAAATTAAAATTAAAT
oCR520	AGTTACTAGTTACCCGGGTTAAACCACGTCTTAAACTTCTCCTGGAACTGAATCTG
oCR521	TTAAGCTTGTACTTAGGAGGATGATTATTTATGGCAACTCCAACATACAC
oCR522	AGTTACTAGTTACCCGGGTTAAACCACGTCCTATTCAGTTGGTTTAAGCGTTGC
oCR523	TTAAGCTTGTACTTAGGAGGATGATTATTTATGCGAAATTTTAAAAATGACAATGAATT
oCR524	AGTTACTAGTTACCCGGGTTAAACCACGTCTTAGCTGGGTAATGGACCTGTA
oCR589	ATTTTAAAAATATCCCACTTTATCCAATTTTCGT
oCR590	ATATATTTATGTTACAGTAATATTGACTTTTAAAAAAGG
oCR591	ACGAAAATTGGATAAAGTGGGATATTTTTAAAATCTGAAATAACCTTCACGCC
oCR592	ATTTAATTTTAATTTTTGTGTTTGTTCCATTTAAATGCCTCCGTTAATTTTTTAATAATTC
oCR593	ATGGAACAAACACAAAAATTAAAATTAAAT
oCR594	TTAAACTTCTCCTGGTACTGAATCTGTTTT
oCR595	AAAACAGATTCAGTACCAGGAGAAGTTTAATAAACAATTAGGAGTGGTAACATGC
oCR596	CCTTTTTTAAAAGTCAATATTACTGTAACATAAATATATGTTGTAGCGTTTAACTGCAAC
oCR597	AAACACTTTTTGGGCTGATAAACCAGGTGCTTACG
oCR598	AAAACGTAAGCACCTGGTTTATCAGCCCAAAAAGT
oCF.36	GCTTTTTCAGATTAGGAGTGATCGTTAAATTTATACTGCAATCG
oCF.37	ATTTAACGATCACTCCTAATCTGAAAAAGCCTCTAATAATTCTTCAAG
oCF.38	GTTTATTTTAATAAAAGCATATATTAAAAATGGAGGGACTTAGAGTTGG
oCF.39	CCTCCATTTTTAATATATGCTTTTATTAAAATAAACTTCTTCGTGATCATG
oCF.40	CAAAATAATTCATGGGGGAGTGATCGTTAAATTTATACTGCAATCG

oCF.41	CGATCACTCCCCCATGAATTATTTTGTTTTTTTTATTTCAATTAC
oCF.42	GGAGGATGATTATTTTTGAAGTACCCTATACGACAAGTAGC
oCF.43	GTATAGGGTACTTCAAAAATAATCATCCTCCTAAGTACAAGCTTAATTG
oCF.70	TCTCACCATCACCATCACCATGGTTCTTCTATGACTATAGATAAGAAAAAATTCATTGAAAAATATGTAAAAGCTTTAGAAAGTAATACA
oCF.72	TCTCACCATCACCATCACCATGGTTCTTCTTTGAAGTACCCTATACGACAAGTAGC
oCF.78	GATCATGATGGTGATTATAAGGATCATGATATCGACTACAAAGACGATGACGACAAGTTGAAGTACCCTATACGACAAGTAGC
oCF.84	CAATTATCTACAGCTAAAAACGAAGATGGCACACCTGT
oCF.85	CTTCGTTTTTAGCTGTAGATAATTGTGCAGTTTCATCGATTTTGTATTCAATTAATTGAG
oCF.86	CATGGTGATGGTGATGGTGAGAAGAACCCATAAATAATCATCCTCCTAAGTACAAGCTTAATTG
oCF.87	GTCTTTGTAGTCGATATCATGATCCTTATAATCACCATCATGATCCTTATAATCCATAAATAATCATCCTCCTAAGTACAAGCTTAATTG
oCF.90	GATAATGTCCAGAAGGTCGATAGAAAGCGTGAGAAACAG
oCF.91	CTTTCTATCGACCTTCTGGACATTATCCTGTACAACATC
oCF.97	CTTGAATGTTCATAAATAATCATCCTCCTAAGTACAAGCTTAATTG
oCF.98	ACTTAGGAGGATGATTATTTATGAACATTCAAGAAGCAACTAAGATAGC
oCF.99	TAAACCACGTCCTATAATTGCTTCAATAATTCCTGGTCTCTAG
oCF.100	ATTATTGAAGCAATTATAGGACGTGGTTTAACCCGGGTAA
oCF.101	TCTCACCATCACCATCACCATGGTTCTTCTATGAACATTCAAGAAGCAACTAAGATAGC
oCF.102	AAGTCTATGATATTGCTATTTCTCATAGTACAAAAGATAAGAAGACAGTTG
oCF.103	TTTTGTACTATGAGAAATAGCAATATCATAGACTTTTTGAGATTGAATATTCTTATT
oCF.104	GGGTTAGTTTTCAAATAGAATACTTTGAAAATCTAAAAAAACCTATATATATAGTAGAGTCTCTTGAAGAATT
oCF.105	GATTTTCAAAGTATTCTATTTGAAAACTAACCCAATCAGATTGAACTGAA
oCF.106	GCGTAAAACAGCAATTTCATATAAATACTCTGAAGCAAAAGATTTAAGA
oCF.107	AGAGTATTTATATGAAATTGCTGTTTTACGCGCCAACTCTAAG
oCF.108	TGGATTGATTGGCAAATAGAATACTCAGTTAAACAAATGAAAAGAGG
oCF.109	CTGAGTATTCTATTTGCCAATCAATCCAATTACTTTCTTTCATATTAGG
oCF.110	TCTCACCATCACCATCACCATGGTTCTTCTTAAGAGTGATCGTTAAATTTATACTGCAATCG
oCF.111	CATGGTGATGGTGATGGTGAGAAGAACCTTTTCTTCTACAGATATTATAATTCGTTGCTTTTT
oCF.112	GGACTTAGAGTTGGCGCGTAAAACATTTATTTCATATAAATAC
oCF.113	TACGCGCCAACTCTAAGTCCCTCCATTTTTAATATATCTAATCTG

oCF.114	GTCTTTGTAGTCGATATCATGATCCTTATAATCACCATCATGATCCTTATAATCTTTTCTTCTACAGATATTATAATTCGTTGCTTTTT
oCF.115	GATCATGATGGTGATTATAAGGATCATGATATCGACTACAAAGACGATGACGACAAGTAAGAGTGATCGTTAAATTTATACTGCAATCG
oCF.116	TCTCACCATCACCATCACCATGGTTCTTCTTAAGAGTGATCGTTAAATTTATACTGCAATCG
oCF.117	CATGGTGATGGTGATGGTGAGAAGAACCTTTTCTTCTACAGATATTATAATTCGTTGCTTTTT
oCF.126	CAGGTGCTTACAAAGTAGGTGAAGGTCAAAAAATCGAAAC
OCF.127	CTTCACCTACTTTGTAAGCACCTGGTTTATCAGCC
oCF.136	TGTGAGCGGATAACAATTATATATTAAAAATGGAGGGACTTAGAGTTGG
oCF.137	CCATTTTTAATATATAATTGTTATCCGCTCACAATTCCAC
oCF.160	GTCTTTGTAGTCGATATCATGATCCTTATAATCACCATCATGATCCTTATAATCCATGCTTTTATTAAAATAAACTTCTTCGTGATCATG

Supplementary Sequences 1. DNA sequences of *mhp* genes from escaper Φ80α-vir phages that avoid Sau-Thoeris immunity. The sequence of the codon for residue V273 is shown in red.

Escaper 1

ATGGAACAAACACAAAAATTAAAATTAAATTTGCAACATTTTGCGAGTAACAATGTTA
AACCGCAAGTATTTAACCCTGATAATGTAATGATGCACGAAAAGAAAGATGGCACG
TTGATGAATGAATTCACAACGCCCATCTTACAAGAGGTTATGGAAAACTCTAAAATT
ATGCAATTAGGTAAGTACGAACCAATGGAAGGTACTGAGAAGAAGTTTACTTTTTG
GGCTGATAAACCAGGTGCTTACTGGGTAGGTGAAGGTCAAAAAATCGAAACATCTA
AAGCTACATGGGTTAATGCTACTATGAGAGCGTTTAAATTAGGGGTTATCTTACCTG
TAACAAAAGAATTCTTGAATTATACTTATTCACAATTCTTTGAAGAAATGAAGCCTAT
GATTGCTGAAGCATTCTATAAAAAGTTTGATGAAGCGGGTATTTTGAATCAAGGTAA
CAATCCATTCGGTAAATCAATTGCGCAATCAATTGAAAAAACTAATAAGGTTATTAA
AGGTGACTTCACACAAGATAACATTATTGATTTAGAGGCATTACTTGAAGATGACGA
ATTAGAAGCAAATGCGTTTATCTCAAAAACACAAAACAGAAGCTTGTTACGTAAAAT
TGTAGATCCTGAAACGAAAGAACGTATTTATGACCGTAACAGTGATTCGTTAGACG
GTCTACCTGTGGTTAACCTTAAATCAAGCAACTTAAAACGTGGTGAATTAATCACTG
GTGACTTCGACAAATTGATTTATGGTATCCCTCAATTAATCGAATACAAAATCGATG
AAACTGCACAATTATCTACAGCTAAAAACGAAGATGGCACACCTGTAAACTTGTTTG
AACAAGACATGGTGGCATTACGTGCAACTATGCATGTAGCATTGCATATCGCTGAT
GATAAAGCGTTTGCTAAGTTAGTTCCTGCTGACAAAAGAACAGATTCAGTTCCAGG
AGAAGTTTAA

Escaper 2

ATGGAACAAACACAAAAATTAAAATTAAATTTGCAACATTTTGCGAGTAACAATGTTA
AACCGCAAGTATTTAACCCTGATAATGTAATGATGCACGAAAAGAAAGATGGCACG
TTGATGAATGAATTCACAACGCCCATCTTACAAGAGGTTATGGAAAACTCTAAAATT
ATGCAATTAGGTAAGTACGAACCAATGGAAGGTACTGAGAAGAAGTTTACTTTTTG
GGCTGATAAACCAGGTGCTTACTGGGTAGGTGAAGGTCAAAAAATCGAAACATCTA
AAGCTACATGGGTTAATGCTACTATGAGAGCGTTTAAATTAGGGGTTATCTTACCTG
TAACAAAAGAATTCTTGAATTATACTTATTCACAATTCTTTGAAGAAATGAAGCCTAT
GATTGCTGAAGCATTCTATAAAAAGTTTGATGAAGCGGGTATTTTGAATCAAGGTAA
CAATCCATTCGGTAAATCAATTGCGCAATCAATTGAAAAAACTAATAAGGTTATTAA
AGGTGACTTCACACAAGATAACATTATTGATTTAGAGGCATTACTTGAAGATGACGA
ATTAGAAGCAAATGCGTTTATCTCAAAAACACAAAACAGAAGCTTGTTACGTAAAAT
TGTAGATCCTGAAACGAAAGAACGTATTTATGACCGTAACAGTGATTCGTTAGACG
GTCTACCTGTGGTTAACCTTAAATCAAGCAACTTAAAACGTGGTGAATTAATCACTG
GTGACTTCGACAAATTGATTTATGGTATCCCTCAATTAATCGAATACAAAATCGATG
AAACTGCACAATTATCTACAGCTAAAAACGAAGATGGCACACCTGTAAACTTGTTTG
AACAAGACATGGTGGCATTACGTGCAACTATGCATGTAGCATTGCATATCGCTGAT
GATAAAGCGTTTGCTAAGTTAGTTCCTGCTGACAAAAGAACAGATTCAGTTCCAGG
AGAAGTTTAA

Escaper 3

ATGGAACAAACACAAAAATTAAAATTAAATTTGCAACATTTTGCGAGTAACAATGTTA
AACCGCAAGTATTTAACCCTGATAATGTAATGATGCACGAAAAGAAAGATGGCACG
TTGATGAATGAATTCACAACGCCCATCTTACAAGAGGTTATGGAAAACTCTAAAATT
ATGCAATTAGGTAAGTACGAACCAATGGAAGGTACTGAGAAGAAGTTTACTTTTTG
GGCTGATAAACCAGGTGCTTACTGGGTAGGTGAAGGTCAAAAAATCGAAACATCTA
AAGCTACATGGGTTAATGCTACTATGAGAGCGTTTAAATTAGGGGTTATCTTACCTG
TAACAAAAGAATTCTTGAATTATACTTATTCACAATTCTTTGAAGAAATGAAGCCTAT
GATTGCTGAAGCATTCTATAAAAAGTTTGATGAAGCGGGTATTTTGAATCAAGGTAA
CAATCCATTCGGTAAATCAATTGCGCAATCAATTGAAAAAACTAATAAGGTTATTAA
AGGTGACTTCACACAAGATAACATTATTGATTTAGAGGCATTACTTGAAGATGACGA
ATTAGAAGCAAATGCGTTTATCTCAAAAACACAAAACAGAAGCTTGTTACGTAAAAT
TGTAGATCCTGAAACGAAAGAACGTATTTATGACCGTAACAGTGATTCGTTAGACG
GTCTACCTGTGGTTAACCTTAAATCAAGCAACTTAAAACGTGGTGAATTAATCACTG
GTGACTTCGACAAATTGATTTATGGTATCCCTCAATTAATCGAATACAAAATCGATG
AAACTGCACAATTATCTACAGCTAAAAACGAAGATGGCACACCTGTAAACTTGTTTG
AACAAGACATGGTGGCATTACGTGCAACTATGCATGTAGCATTGCATATCGCTGAT
GATAAAGCGTTTGCTAAGTTAGTTCCTGCTGACAAAAGAACAGATTCAGTTCCAGG
AGAAGTTTAA

Escaper 4

ATGGAACAAACACAAAAATTAAAATTAAATTTGCAACATTTTGCGAGTAACAATGTTA
AACCGCAAGTATTTAACCCTGATAATGTAATGATGCACGAAAAGAAAGATGGCACG
TTGATGAATGAATTCACAACGCCCATCTTACAAGAGGTTATGGAAAACTCTAAAATT
ATGCAATTAGGTAAGTACGAACCAATGGAAGGTACTGAGAAGAAGTTTACTTTTTG
GGCTGATAAACCAGGTGCTTACTGGGTAGGTGAAGGTCAAAAAATCGAAACATCTA
AAGCTACATGGGTTAATGCTACTATGAGAGCGTTTAAATTAGGGGTTATCTTACCTG
TAACAAAAGAATTCTTGAATTATACTTATTCACAATTCTTTGAAGAAATGAAGCCTAT
GATTGCTGAAGCATTCTATAAAAAGTTTGATGAAGCGGGTATTTTGAATCAAGGTAA
CAATCCATTCGGTAAATCAATTGCGCAATCAATTGAAAAAACTAATAAGGTTATTAA
AGGTGACTTCACACAAGATAACATTATTGATTTAGAGGCATTACTTGAAGATGACGA
ATTAGAAGCAAATGCGTTTATCTCAAAAACACAAAACAGAAGCTTGTTACGTAAAAT
TGTAGATCCTGAAACGAAAGAACGTATTTATGACCGTAACAGTGATTCGTTAGACG
GTCTACCTGTGGTTAACCTTAAATCAAGCAACTTAAAACGTGGTGAATTAATCACTG
GTGACTTCGACAAATTGATTTATGGTATCCCTCAATTAATCGAATACAAAATCGATG
AAACTGCACAATTATCTACAGCTAAAAACGAAGATGGCACACCTGTAAACTTGTTTG
AACAAGACATGGTGGCATTACGTGCAACTATGCATGTAGCATTGCATATCGCTGAT
GATAAAGCGTTTGCTAAGTTAGTTCCTGCTGACAAAAGAACAGATTCAGTTCCAGG
AGAAGTTTAA

Wild-type

ATGGAACAAACACAAAAATTAAAATTAAATTTGCAACATTTTGCGAGTAACAATGTTA
AACCGCAAGTATTTAACCCTGATAATGTAATGATGCACGAAAAGAAAGATGGCACG
TTGATGAATGAATTCACAACGCCCATCTTACAAGAGGTTATGGAAAACTCTAAAATT

ATGCAATTAGGTAAGTACGAACCAATGGAAGGTACTGAGAAGAAGTTTACTTTTTG
GGCTGATAAACCAGGTGCTTACTGGGTAGGTGAAGGTCAAAAAATCGAAACATCTA
AAGCTACATGGGTTAATGCTACTATGAGAGCGTTTAAATTAGGGGTTATCTTACCTG
TAACAAAAGAATTCTTGAATTATACTTATTCACAATTCTTTGAAGAAATGAAGCCTAT
GATTGCTGAAGCATTCTATAAAAAGTTTGATGAAGCGGGTATTTTGAATCAAGGTAA
CAATCCATTCGGTAAATCAATTGCGCAATCAATTGAAAAAACTAATAAGGTTATTAA
AGGTGACTTCACACAAGATAACATTATTGATTTAGAGGCATTACTTGAAGATGACGA
ATTAGAAGCAAATGCGTTTATCTCAAAAACACAAAACAGAAGCTTGTTACGTAAAAT
TGTAGATCCTGAAACGAAAGAACGTATTTATGACCGTAACAGTGATTCGTTAGACG
GTCTACCTGTGGTTAACCTTAAATCAAGCAACTTAAAACGTGGTGAATTAATCACTG
GTGACTTCGACAAATTGATTTATGGTATCCCTCAATTAATCGAATACAAAATCGATG
AAACTGCACAATTATCTACAGTTAAAAACGAAGATGGCACACCTGTAAACTTGTTTG
AACAAGACATGGTGGCATTACGTGCAACTATGCATGTAGCATTGCATATCGCTGAT
GATAAAGCGTTTGCTAAGTTAGTTCCTGCTGACAAAAGAACAGATTCAGTTCCAGG
AGAAGTTTAA